Research Square

Preprints are preliminary reports that have not undergone peer review. They should not be considered conclusive, used to inform clinical practice, or referenced by the media as validated information.

Antiproliferative Activity of New Neocryptolepine–Rhodanine–α-Aminophosphonate Conjugates: In Vitro and In Silico Evaluation

Hanem M. Awad
National Research Centre

Abdullah A. S. Ahmed
Menoufia University

Yasmine S. Moemen
National Liver Institute, Menoufia University

Mohamed Aly
Tianjin University

Ahmed I. El-Tantawy
Okayama University

Elshaymaa I. Elmongy
Capital University

Ibrahim El Sayed
ibrahimtantawy@science.menofia.edu.eg

Menoufia University

Article

Keywords: Neocryptolepine, Rhodanine, Alpha amino phosphonate, Anticancer, Molecular docking

Posted Date: October 15th, 2026

DOI: https://doi.org/10.21203/rs.3.rs-11077561/v1

License: This work is licensed under a Creative Commons Attribution 4.0 International License. Read Full License

Additional Declarations: No competing interests reported.

Antiproliferative Activity of New Neocryptolepine–Rhodanine–α-Aminophosphonate Conjugates: *In Vitro* and *In Silico* Evaluation

Hanem M. Awad [a*], Abdullah A. S. Ahmed [b], Yasmine S. Moemen [c], Mohamed Aly Saad Aly [d], Ahmed I. El-Tantawy [e], Elshaymaa I. Elmongy [f], and Ibrahim El Tantawy El Sayed [b*]

[a] Department of Tanning Materials and Leather Technology, National Research Centre, Dokki, Giza 12611, Egypt
[b] Chemistry Department, Faculty of Science, Menoufia University, Shebin El-Kom 32511, Egypt
[c] Clinical Pathology Department, National Liver Institute, Menoufia University, Shebin El-Kom 32511, Egypt
[d] Department of Electrical and Computer Engineering at Georgia Tech Shenzhen Institute (GTSI), Tianjin University. Shenzhen, Guangdong, 518055, China.
[e] Research Institute for Interdisciplinary Science, Okayama University, Tsushima-naka, Kita-ku, Okayama 700-8530, Japan
[f] Department of Pharmaceutical Chemistry, Faculty of Pharmacy, Capital University (formerly Helwan), Ain Helwan,

Corresponding authors:
Ibrahim El Tantawy El Sayed, ibrahimtantawy@science.menofia.edu.eg

Abstract: In the current study, eight novel conjugates were synthesized as natural-based heterocyclic compounds bearing a neocryptolepine pharmacological core modified by bioactive moieties of rhodanine and α- aminophosphonate, thus emphasizing the benefits of hybridization. The antiproliferative activity of all conjugates was evaluated against HCT-116, HepG-2, MCF-7, and A549 cancer cell lines in addition to a normal cell line (RPE-1). Most of the derivatives displayed antiproliferative activity against all tested cancer cell lines, more than the control drug, Doxorubicin. Furthermore, a strong indication of the synergistic antiproliferative effect of the conjugates as compared to their precursors was observed. Among all conjugates, conjugate **12a** showed the highest activity against HCT-116, MCF-7 and A549, with IC_{50}: 0.1, 7.4, and 17.4 μM, while **12d** was the best against HepG-2, with IC_{50} 19.4 μM. it is worth mentioning that most of the synthesized conjugates have low toxicity towards RPE-1 normal cells, in particular **12a,** which has the highest selectivity index values. Molecular docking studies were conducted against topoisomerases I and II. Notably, the binding affinities were almost consistent with the biological results, recording the best binding energy for topoisomerase I by **12a**, while in topoisomerase II, the lowest binding energies were observed in **11d** and **12a,b**.

Keywords: Neocryptolepine; Rhodanine; Alpha amino phosphonate; Anticancer; Molecular docking

Introduction

The emergence of uncontrolled growth of cancer cells and the increasing death numbers, according to WHO reports, alert many researchers to develop and discover new, safe therapy aiming to face this immense disease [1]. Different types of therapies, including immunotherapy, radiotherapy, gene therapy and molecular targeted therapy, are applied as a cure for cancer [2]. Among these techniques, chemotherapy is a persistent treatment for cancer despite its toxic side effects [3]. From the above-mentioned, continuous efforts were carried out to find anticancer drugs with minimum side effects. Nature reveals vast naturally occurring pharmaceutical compounds with potent biological activities, inspiring many researchers to synthesize and develop many natural-based drugs as Taxol and chloroquine, applicable for the treatment of many disorders [4]. It is worth recalling that heterocyclic compounds are widely used in chemistry and biosciences, playing a crucial role in human biological systems [5-7]. In addition, heterocyclic compounds, including two-, three-, and four-fused rings, have received great concern regarding their marvellous biological activities as well as their capability to structural modifications on their different active sites [8-10]. Rhodanine I, an uracil mimic, is a small heterocyclic compound as shown in Figure 1 has significant biological activities, including anticancer, antimicrobial, and antidiabetic agents [11-13]. The hydrogen bond donor/acceptor binding sites on rhodanine ring, as well as π-π stacking, would enhance DNA intercalation and enzyme inhibition, such as Aldose Reductase (ALR2), and Protein Tyrosine Phosphatase 1B (PTP1B). This has led to the development of diverse drug-like molecules [14]. On the same trend, naturally occurring indoloquinoline such as neocryptolepine II (Figure 1) has widespread uses in medicinal chemistry owing to its potent activity against different diseases such as malaria and cancer [15-17]. It is worth remembering that neocryptolepine alkaloids are present in the root *Cryptolepis sanguinolenta* with other regioisomeric alkaloids such as cryptolepine and isocryptolepine [18]. The variety of the orientation and binding sites of indole and quinoline influences the biological activity of these alkaloids. The planarity of neocryptolepine facilitates DNA intercalation, especially for GC-rich sequences, through π-π stacking interactions, resulting in a potent DNA topoisomerase inhibitor [19-21]. Moreover, α-aminophosphonates III are key intermediates in the synthesis of many biologically active compounds. They play a significant role in medicinal chemistry applications and drug therapy. They structurally resemble the natural α-amino acids, the "building blocks" of peptides and proteins [22-24]. Because of their crucial role in biological activity, metabolic stability, and low toxicity to mammalian cells, broad capability of influencing physiologic and pathologic processes, α-aminophosphonates have garnered a lot of attention [25]. The Kabachnik–Fields reaction is the most convenient method for the preparation of α-aminophosphonates III [26]. This reaction is based on a three-one-pot component strategy by the reaction of aldehydes or ketones with primary amines and phosphite in the presence of a Lewis acid catalyst such as $LiClO_4$ or $Cu(OTf)_2$. On the other

hand, the Pudovik reaction involves the phosphorus-hydrogen addition of dialkyl/aryl phosphite to Schiff base compounds [27].

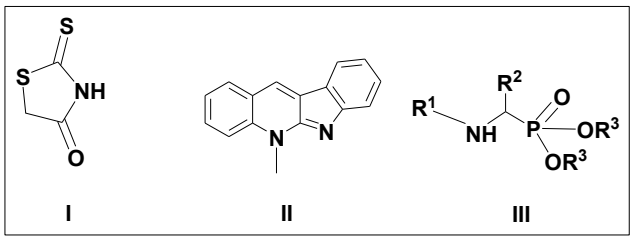

Figure 1: Structures of rhodanine I, neocrytolepine II, and α -aminophosphonates III

Recently, molecular hybridization has emerged a powerful strategy in the design and development of novel drugs. This approach provides novel way to synthesize new candidates for treating a wide range of diseases, including cancer. A common approach is to merge multiple pharmacophores into a single multifunctional molecule using a linker chain. This new molecule can interact with multiple targets, boosting its biological activity while reducing the side effects linked to each component and minimizing potential drug interactions [28-30]. In this context, neocryptolepine serves as a distinctive motif for developing diverse classes of biologically active analogues that exhibit a broad spectrum of pharmacological proprieties, such as anticancer [31], antimalarial [32] and antiplasmodial activity [33]. Recent studies revealed that the hybridization of neocryptolepine at the C-11 position with rhodanine as well as acridine have synergistic effect on biological activity [34]. The broad therapeutic potential of neocryptolepine, rhodanine and aminophosphonate, along with their related analogues inspired us to investigate conjugated leads combining all these pharmacological entities in a single hybrid molecular target has been utilized as a promising drug design strategy for synergistic anticancer effect with site-specificity. Possible modifications to the neocryptolepine core structure II (*cf.* Figure 2) aimed at enhancing anticancer activity include adding various side chains at position 11. The choice of spacer and its substitutions can affect the structure's flexibility, which may either weaken or strengthen interactions with specific target biomolecules. Such modifications in the molecular structure can significantly influence and enhance biological activity. Based on that, this study demonstrated the incorporation of biologically active N-containing scaffold rhodanine I, and aminophosphonate III into the neocryptolepine structure II, aiming to enhance the neocryptolepine pharmacological properties as an anticancer candidate with a synergistic effect when compared to the individual moieties, as shown in Figure 2. The current study focuses on the design and development of urgently needed and highly effective new conjugates of neocryptolepine bearing an aminophosphonate scaffold with a rhodanine congener, as depicted in Figure 2, and further evaluation of their anti-proliferative activity against different human cell lines. Additionally,

a molecular docking study was conducted to verify the binding of synthesized conjugates with the target protein, providing valuable insights into their potential mechanisms of action.

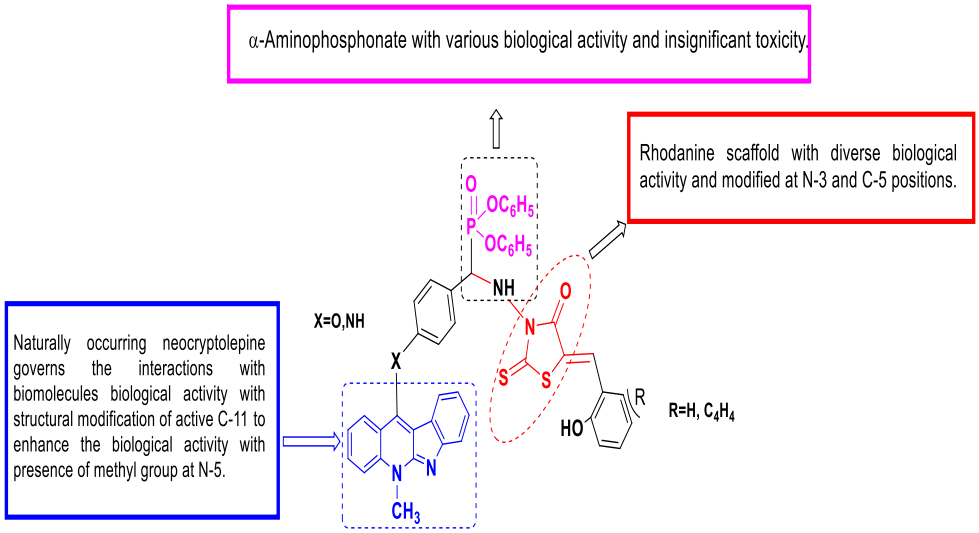

Figure 2: Schematic diagram for the design of neocrytptolepine, rhodanine and aminophosphonate conjugates.

Results and Discussion

Chemistry:
Synthesis of 11-chloro neocryptolepine 1

Preparation of 11-chloroneocryptolepine required multistep reactions, starting with 1, as previously reported in the literature [19].

Aldehydes bearing neocryptolepine core Preparation (3)

According to the reported method [22], the reaction of 11-chloro neocryptolpine 1 with 4-hydroxy or amino benzaldehyde 2a,b in the presence of potassium carbonate anhydrous and Dimethyl formamide (DMF) under reflux condition to give 11-formyl neocryptolpine derivatives 3a,b in good yields (76%) via nucleophilic substitution reaction (SN_{Ar}), as shown in **Scheme1.**

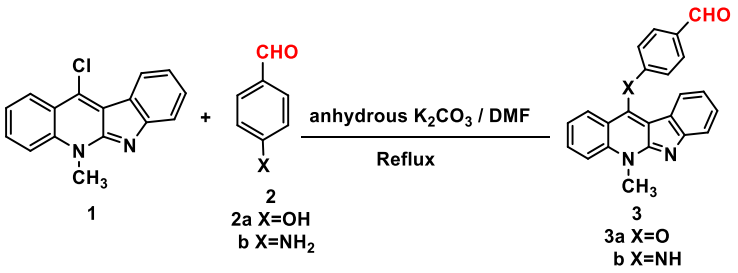

Scheme 1. Synthesis of aldehyde bearing neocryptolpine core 3

According to the literature [22], The formation of **3b** via spectroscopic methods. In the FTIR spectrum of **3b**, an intense absorption band at υ:1666 cm^{-1} was assigned to the characteristic formyl (CHO) group. In addition, a singlet with a chemical shift at δ: 9.55 ppm was seen in the ^{1}H NMR spectrum of **3b**, which corresponds to the aldehydic proton. The ^{13}C NMR spectrum for compound **3b** showed further confirmation of the existence of an aldehydic group, with a peak at δ: 190.68 ppm.

Synthesis of neocryptolepine-rhodanine congers 7a-d and 9a-d

The synthetic approach of neocryptolepine-rhodanine congers **7a-d** and **9a-d** initiated by the condensation of aldehydes **3** or **6** with *N*-aminorhodine **4** in ethanol with the addition of a few drops of glacial acetic acid under reflux yields the corresponding Schiff-bases **5a,b** or **8a, b**, previously reported in the literature [35, 36] with good yields. Further Knoevenagel condensation reaction was carried out on the obtained Schiff bases **5** or **8** by reaction with aldehydes **6** or **3,** respectively, in the presence of sodium acetate to afford the corresponding **7a-d** and **9a-d** in high yields as depicted in **Scheme 2**.

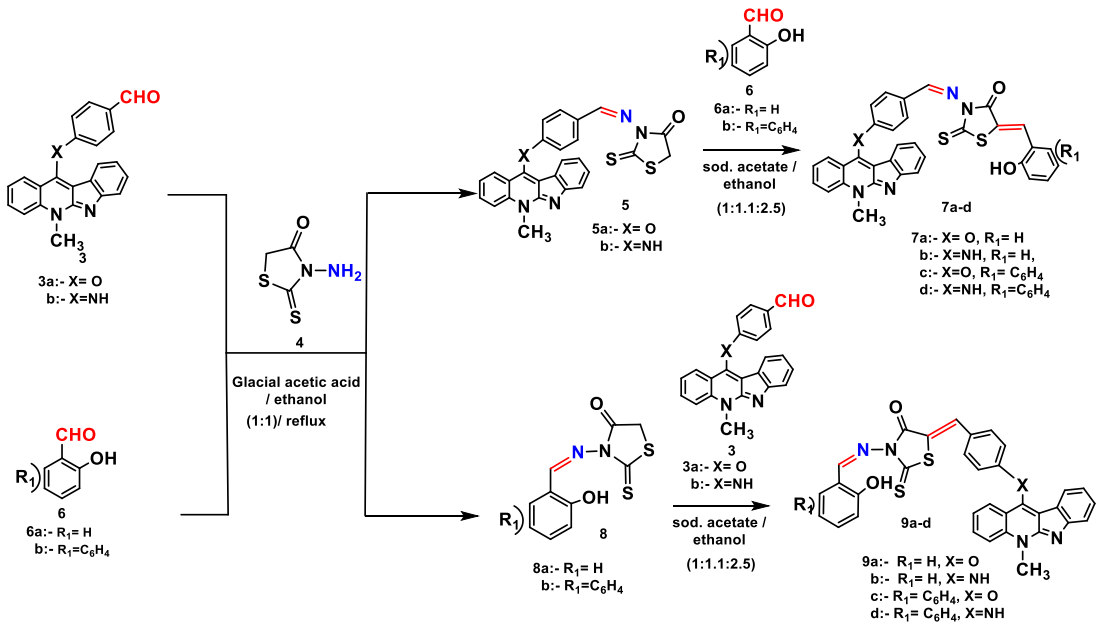

Scheme2. Synthesis of neocryptolpine-rhodanine congers **7a-d** and **9a-d**

FTIR spectra exhibiting the absorption peak of Schiff base (CH=N) at υ: 1573 and 1581 cm^{-1} corresponding to **5a** and **5b**, respectively. The ^{1}H NMR spectra recorded a distinctive signal for the (C<u>H</u>=N) protons, which appeared at δ: 8.48 and 8.95 ppm for **5a** and **5b** in succession confirming the formation of Schiff bases **5a** and **5b**. Additionally, the active methylene protons (C<u>H</u>$_2$) appeared at δ: 5.94 and 5.71 ppm for **5a** and **5b**, respectively. Meanwhile, ^{13}C NMR spectra revealed the presence of the active methylene carbon (<u>C</u>H$_2$) signals bearing the rhodanine ring at

δ: 47.04 and 45.24 ppm of **5a** and **5b,** respectively. Furthermore, (CH=N) carbon signals for **5a** and **5b** were recorded at δ:147.49 and 147.39 ppm. In addition, the mass spectra of the synthesized Schiff bases reported the molecular ion peaks in coincidence with their expected values. **8a** and **8b**'s spectral findings were in line with what was already known from the reported literature [35, 36]. On the other hand, the FTIR spectra of **7a-d** and **9a-d**, revealing the olefinic (CH) stretching at υ: 3055 cm^{-1} for **7a**, **7c** and **7d**, besides υ:3047 cm^{-1} for **7b** meanwhile, the olefinic (CH) appeared at υ: 3062 cm^{-1} for **9a**, 3047 cm^{-1} for **9b**, 3055 cm^{-1} for **9c** and 3047 cm^{-1} for **9d**. In addition, the EI-MS spectra of **7a-d** and **9a-d** showed data consistent with their expected values. Alternatively, the appearance of the olefinic proton of the exocyclic bond (C<u>H</u>=C) from a value of δ: 7.92 to 8.11 ppm on the expense of the disappearance of the ring methylene proton (C<u>H</u>$_2$) confirmed the installation of **7a-d** and **9a-d**. It is important to keep in mind that the stereochemistry of the double bond favors the geometry of the *Z* over the *E* as in isomers [37-39]. This was demonstrated by the fact that the downfield shift of the olefinic proton observed at δ: 7.94, 8.11, 8.03, and 7.96 ppm overlapped with the (CH_{Ar}) proton for congeners **7a**, **7b**, **7c**, and **7d**, respectively. This pattern was detected in their regioisomers **9**, in which the olefinic proton was observed at δ: 7.92, 7.94, 8.01, and 8.07 ppm for **9a**, **9b**, **9c**, and **9d**, respectively.

Synthesis of α-aminophosphonate conjugates containing neocryptolepine-rhodanine congers 11a-d and 12a-d.

Eventually, the installation of α-aminophosphonate conjugates incorporating neocryptolepine-rhodanine scaffolds **11a-d** and **12a-d was** obtained by the nucleophilic P-H addition of diphenyl phosphite **10** to (CH=N) bearing **7a-d** or **9a-d** with good yields via the Pudovik reaction as depicted in **Scheme 3**.

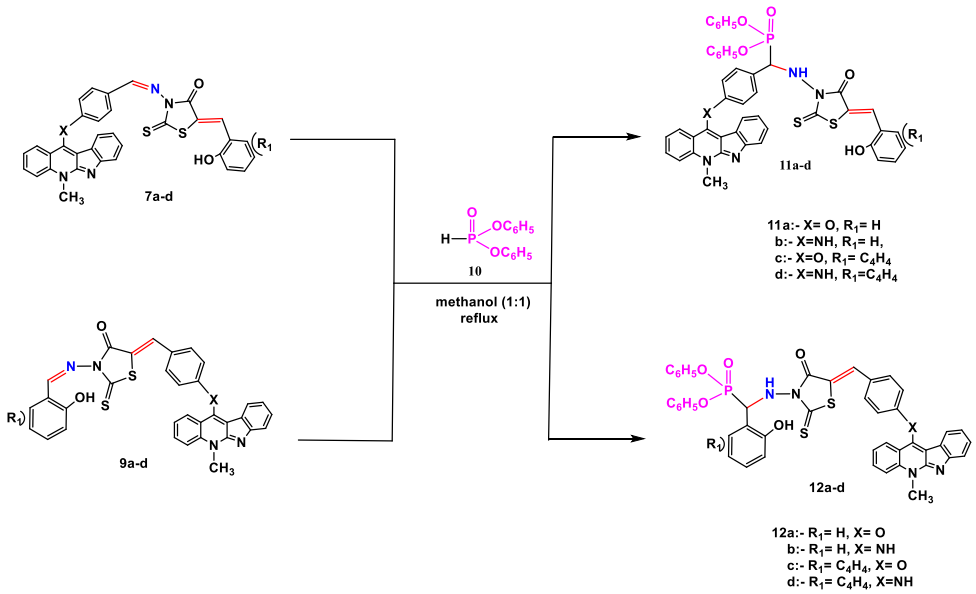

Scheme3. Synthesis of α-aminophosphonate conjugates **11a-d** and **12a-d**.

The characterization of the target α-aminophosphonate conjugates **11a-d** and **12a-d** was confirmed using FTIR, NMR and EI-MS analysis. The FTIR spectra for both **11** and **12** displayed distinctive peaks for (NH) at the following υ: 3410 cm^{-1} for **11a**, 3417 cm^{-1} for **11b**, and 3425 cm^{-1} for **11c** and **11d** as well as at 3441 cm^{-1} for **12a**, 3425 cm^{-1} for **12b**, 3417 cm^{-1} for **12c**, and 3404 cm^{-1} for **12d**. In addition, ^{1}H NMR spectra exhibited chiral proton signals for (C<u>H</u>-P) of **11a-d** & **12a-d** at δ: 6.73 ppm, except for **11c** at δ: 6.78 ppm as a doublet, which confirmed the formation of α-aminophosphonates at the expense of the removal of the (CH=N) peak. Moreover, the ^{13}C NMR spectra demonstrated that the chiral carbon of (<u>C</u>H-P) ranged from δ: 54.15 to 58.50 ppm. Finally, the EI-MS spectra of **11a-d** and **12a-d** recorded molecular ion peaks of the synthesized conjugates with their expected values.

The following is an example of a proposed mechanism for the synthesis of α-aminophosphonate conjugates bearing aldehyde–rhodanine congers: The elimination of water is the initial stage in the process, which takes place during the interaction of aldehydes with *N*-amino rhodanine in the presence of glacial acetic acid. This resulted in the formation of the Schiff base. The next step is the Knoevenagel condensation reaction, which involves activating the methylene group on *N*-amino rhodanine using sodium acetate as a catalyst, attacking the carbon atom of aldehyde derivatives, and removing the water to produce aldehyde-rhodanine conjugates. In addition, by adding a phosphorus-hydrogen bond across the imine double bond, it is possible to produce conjugates **11a-d** and **12a-d**, as shown in **Scheme 4**.

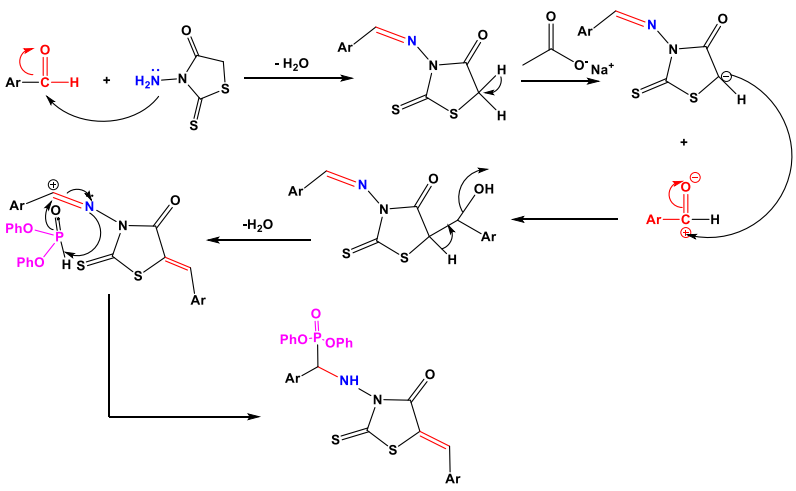

Scheme 4. Proposed mechanism of neocryptolepine-α- aminophosphonate conjugates **11a-d** and **12a-d**

Antiproliferative screening

All synthesized compounds were evaluated for their ability to inhibit the growth of HCT-116, MCF-7, HepG2, and A549 cancer cell lines, to assess their cytotoxicity using the MTT assay. The percentage of viable cells was compared to the control. Each of the four cancer cell lines was tested, and the efficacy of the compounds was measured against the reference drug, Doxorubicin. All compounds demonstrated a dose-dependent inhibition of growth across the four human cancer cell lines; results are tabulated in **Table-1.**

Table 1: IC_{50} values of the compounds against the four cancer types and normal cell line (RPE-1) in MTT assay

	IC_{50} (µM) ± SEM				
No.	HCT-116	MCF-7	HepG2	A549	RPE-1
1	5.2 ± 1.3	13.1 ± 3.2	25.2 ± 2.7	19.6 ± 2.9	24.9 ±3.3
2a	5.7 ± 1.2	26.6 ± 3.5	28.1 ± 3.5	20.6 ± 3.1	27.7 ±3.3
2b	8.6 ± 1.7	26.3 ± 3.7	27.3 ± 2.7	26.7 ± 3.5	31.6 ±3.6
3a	6.2 ± 1.5	20.6 ± 2.9	21.6 ± 2.7	21.5 ± 2.3	25.1 ±3.3
3b	4.7 ± 1.2	17.0 ± 2.9	24.0 ± 3.3	22.1 ± 2.1	20.0 ±2.9
4	12.3 ± 1.9	29.0 ± 3.8	25.8 ± 3.3	23.1 ± 2.5	31.7 ±3.2

5a	14.9 ± 2.7	24.7 ± 3.7	23.5 ± 2.7	23.9 ± 2.5	31.4 ±2.3
5b	18.8 ± 2.6	20.5 ± 3.1	26.7 ± 3.3	27.2 ± 3.4	20.5 ±3.1
6a	13.7 ± 2.1	28.1 ± 3.6	36.0 ± 4.1	37.0 ± 4.6	33.9 ±3.5
6b	6.8 ± 1.5	15.5 ± 2.2	26.9 ± 3.8	25.7 ± 3.2	23.3 ±3.2
7a	15.9 ± 2.4	18.7 ± 3.1	22.8 ± 3.1	24.4 ± 2.1	26.4 ±3.3
7b	15.1 ± 2.1	18.6 ± 2.9	24.5 ± 3.1	24.9 ± 3.3	21.6 ±2,9
7c	12.1 ± 2.1	10.8 ± 1.5	23.1 ± 2.7	21.5 ± 2.6	19.6 ±3.5
7d	16.9 ± 2.8	25.2 ± 3.5	26.7 ± 3.7	34.7 ± 4.5	20.7 ±3.3
8a	9.2 ± 1.5	25.3 ± 3.7	23.8 ± 2.9	22.1 ± 3.1	33.6 ±3.6
8b	4.6 ± 1.2	13.4 ± 2.9	32.2 ± 3.9	26.0 ± 3.1	22.3 ±2.0
9a	6.7 ± 1.4	19.2 ± 3.1	23.0 ± 3.2	21.9 ± 2.5	20.6 ±3.3
9b	10.0 ± 1.9	18.7 ± 2.8	23.4 ± 3.1	24.9 ± 3.1	22.5 ±3.6
9c	13.8 ± 1.5	19.8 ± 3.1	27.0 ± 2.9	26.6 ± 3.2	42.0 ±3.1
9d	11.0 ± 2.1	17.2 ± 2.8	22.1 ± 3.1	21.9 ± 2.7	24.5 ±2.9
11a	17.7 ± 2.2	14.1 ± 2.1	23.3 ± 2.5	21.9 ± 2.9	23.2 ±3.2
11b	7.5 ± 1.7	24.1 ± 3.7	26.8 ± 3.1	24.9 ± 3.7	40.5 ±3.6
11c	23.4 ± 3.1	20.7 ± 2.7	26.5 ± 2.9	31.0 ± 3.8	20.6 ±3.3
11d	5.5 ± 1.1	22.9 ± 2.9	23.9 ± 3.1	22.4 ± 3.3	31.8 ±2.3
12a	0.1 ± 0.05	7.4 ± 1.5	27.5 ± 3.9	17.4 ± 2.3	17.4 ±3.3
12b	3.7 ± 1.1	11.1 ± 1.9	24.5 ± 3.4	24.5 ± 3.1	19.1 ± ±3.5
12c	14.3 ± 1.8	17.7 ± 3.1	22.9 ± 3.9	20.0 ± 2.5	32.5 ±3.3
12d	15.6 ± 2.1	18.2 ± 3.2	19.4 ± 3.1	19.7 ± 2.8	32.6 ±3.6
Dox.	10.9 ± 2.3	26.5 ± 3.7	32.8 ± 3.6	27.9 ± 4.1	25.1 ±2.9

Compared to Doxorubicin and against colon cancer cells HCT116, conjugate **12a** showed the best antiproliferative activity with IC_{50}: 0.1 µM followed by **12b,** then **11d** and **11b** with IC_{50s}: 3.7, 5.5, and 7.5 µM, which are better values than those recorded by the reference drug (IC_{50}: 10.9 µM). However, all series **11a-d** and **12a-d** recorded better antiproliferative activity than the reference Doxorubicin against breast cancer cells MCF-7, among which conjugate **12a** and **12b** were the best, recording IC_{50} values of 7.4 and 11.1 µM, respectively. Regarding hepatic cancer cells (HepG2), all compounds recorded better cytotoxicity than Doxorubicin, especially **12d** has the best antiproliferative activity (IC_{50}19.4 µM)**.** Analyzing the results against lung cancer cell (A549), all compounds except **11c** were more cytotoxic than Doxorubicin, and conjugate **12a** was the best among all with $IC_{50:}$ 17.4 µM followed by **12d** that recorded IC_{50}: 19.7 µM.

Selectivity index: against normal cell -Human retinal pigment epithelial-1 (RPE-1)

To assess the anticancer properties of the compounds, a selectivity assay was conducted to determine their preference for malignant cells, reflected by their selectivity index (SI). The SI was calculated as the ratio of the IC_{50} value for the selected compounds on normal cell -Human retinal pigment epithelial-1 (RPE-1) to the IC_{50} value on the four tested cancer cells. Compounds with an SI exceeding 3 were identified as potentially selective for cancer cells [40]. From the tabulated results in Table 1, thirteen compounds were found to have anticancer activity with a selectivity index exceeding 3 in the ratio between the recorded IC_{50} values of the normal cell RPE-1 to colon cancer cell HCT 116. However, among the synthesized aminophosphonate conjugates 11a-d and 12a-d and their rhodanine congers 7a-d and 9a-d, conjugate 12a showed the best selectivity with SI of 17.4 followed by 11d, 11b, 12b, 9a and 9c with SI values of 5.78, 5.40, 5.16, 3.07 and 3.04 respectively, **Chart 1**. It is worth noting that the selectivity of the reference drug was lower than most of the synthesized compounds.

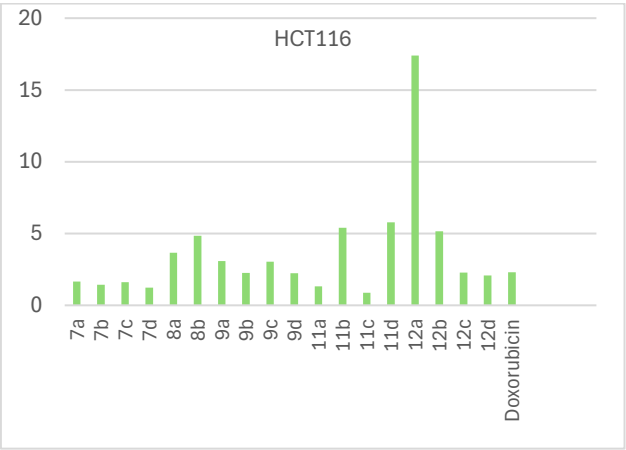

Chart 1: SI values of compounds 7a-d, 9a-d and their conjugates 11a-d and 12a-d

Study of structure-activity relationships (SARs) of neocryptolepine conjugates 11 and 12:

In this work, the structure of the pharmacological core, neocryptolepine, was modified through chemical hybridization in order to increase its biological activity. The alteration of the neocryptolepine core at the C-11 position was implemented through the interaction with bioactive cores such as rhodanine and aminophosphonates. In addition, further modification was applied to the C-5 of the rhodanine ring by addition of phenyl or naphthyl groups as linkers, aiming to enhance the biological activity as an antiproliferative agent. Notably, the modification of the C-5 position of the rhodanine core is among the traditional steps in drug discovery for the generation of new analogues with potent activity, where the aim is to access a precise area or dense regions of chemical space to modulate the biochemical pathways [41]. The rationale behind the rhodanine core structural modification at the C-5 position is to improve the selectivity and/or efficacy using functionalized hydroxy-substituted aldehydes such as salicylaldehyde **6a** and 2-hydroxy-1-naphthaldehyde **6b** to generate analogues with an extra drug target binding site, such as the hydroxy (OH) pharmacophore, with hydrogen bonding donor/ acceptor binding mode with drug targets such as proteins. Additionally, the exocyclic double bond and aryl group at the C-5 position of the rhodanine scaffold provide extra hydrophobic binding sites on the target protein's surface, potentially enhancing or weakening interactions with specific biomolecules. Moreover, the presence of phenoxy or amino group at C-11 of neocryptolepine would increase the likelihood that the aldehyde bearing neocryptolepine core would interact with other molecules or boost the ability of the oxygen or nitrogen atom to create hydrogen bonds.

The model of synergistic effect for the synthesized conjugates from their parents was represented by the establishment of **12a.** For the formation of **12a**, it was initiated with the addition of *N*-amino rhodanine **4** to salicylaldehyde **6a** to form Schiff base **8a** we noted the synergistic effect illustrated by the enhancement of IC_{50} against HCT-116, MCF-7 and A549 respectively form 13.7, 28.1 and 37.0 μM for **6a** to 9.2, 25.3 and 22.1 μM for **8a.** Further improvement on IC_{50} of **8a** was performed by addition of phenoxy neocryptolepine as a linker at C-5 of rhodanine core, one of the promising sites enhanced the biological activity, to form **9a** with IC_{50} 6.7, 19.2 and 21.9 μM. The P-H addition via diphenyl phosphite **10** to **9a** to form **12a** with IC_{50}: 0.1, 7.4 and 17.4 μM towards HCT-116, MCF-7 and A549 respectively. At the same time, this conjugate also has higher activity than the reference drug doxorubicin against different cancer cell lines as illustrated in **Table 2**

Table 2: synergistic potency of **12a** against HCT-116, MCF-7, and A549

No	Compound	IC_{50} µM (HCT-116)	IC_{50} µM (MCF-7)	IC_{50} µM (A549)
4	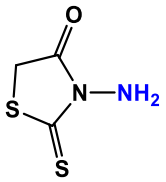	12.3	29.0	23.1
6a	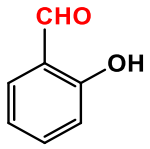	13.7	28.1	37.0
8a	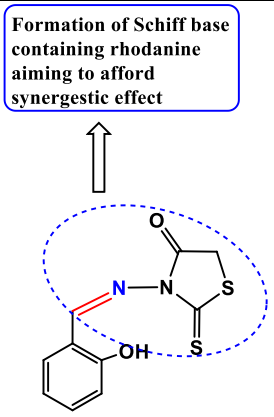	9.2	25.3	22.1
9a	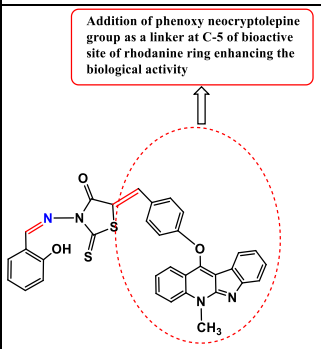	6.7	19.2	21.9
12a	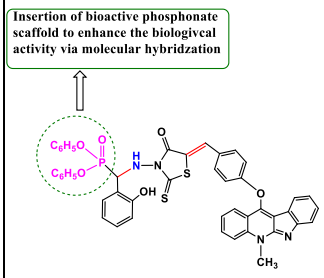	0.1	7.4	17.4

To demonstrate the concept of the enhancement of antiproliferative activity *via* structural modification through increasing the pharmacophoric cores or addition of linkers from the obtained values of IC_{50}. In the case of conjugate **12b** against HCT -116 cancer cell line, we noticed the IC_{50} value of **8a** at 9.2 µM was enhanced throughout the hybridization of their parents of salicylaldehyde **6a** and N-amino rhodanine **4** with IC_{50} of 13.7 and 12.3 µM respectively. Unfortunately, after the addition of 11-formyl neocryptolepine containing amino group **3b** at C-5 of changed the IC_{50} value from 9.2 to 10.0 µM represented to **9b**. Meanwhile, the addition of phosphonate scaffold to conjugate **12b** containing three pharmacophoric cores of neocryptolepine, rhodanine and aminophosphonate enhanced the IC_{50} value from 10.0 to 3.7 µM.

On the same trend, the effect of molecular hybridization also turns out to conjugate **12b** against MCF-7. The improvement of Schiff base **8a** with IC_{50} 25.3 µM was observed comparing to its scaffolds of salicylaldehyde **6a** and *N*-amino rhodanine **4** with IC_{50} 28.1 and 29.0 µM respectively. Furthermore, the addition of a phenyl group attached to hydroxyl group as a linker at C-5 of rhodanine changed the IC_{50} to 18.7 µM compared to **9b,** but higher than its precursor **3b** with IC_{50} 17.0 µM. Whereas the insertion of a phosphonate scaffold into conger **9b** enhanced the IC_{50} of **12b** with IC_{50} 11.1 µM, emphasizing the role of molecular hybridization in optimization of biological activity. Notably, the formed **12b** has greater antiproliferative activity than the reference drug and its precursors, as shown in **Table 3.**

Table 3: synergistic potency of **12b** against HCT-116, MCF-7, and A549

No	Compound	IC_{50} (HCT-116)	IC_{50} (MCF-7)
4	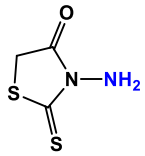	12.3	29.0
6a	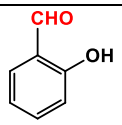	13.7	28.1
8a	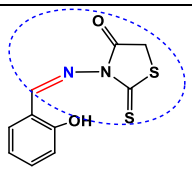	9.2	25.3

9 b	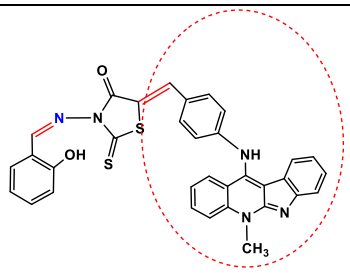	10.0	18.7
12 b	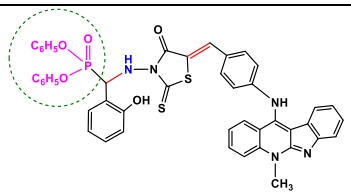	3.7	11.1

Comparison between the antiproliferative activity of conjugate 11a-d and 12a-d

When tested against the **HCT-116** cancer cell line for the afforded conjugates **11a-d** and **12a-d**, it was found that the location of the phenoxy group of the neocryptolepine core located at position C-5 of the rhodanine ring in conjugate **12a** was more effective than the same group located as Schiff base at position N-3 of rhodanine ring in conjugates **11a**. The presence of a neocryptolepine-aldehyde containing amino group **3b** at position N-3 of the rhodanine ring in conjugate **11b** is associated with a reduced anticancer activity when compared to the presence of the same group at position C-5 of the rhodanine ring in conjugate **12b**. Similarly, conjugate **11c**, which contains a phenoxy group bearing a neocryptolepine core at N-3 of rhodanine ring in Schiff base form, shows a reduction in cytotoxic effect when compared to its regio-isomer **12c**, which has the same group linked to the rhodanine ring at C-5. However, conjugate **11d**, which contains naphthyl associated with a hydroxyl group at C-5 of the rhodanine ring, exhibits greater anticancer activity than **12d**. Additionally, The observation of The IC_{50} of the aforementioned conjugates **12a-d**, in comparison to regio-isomers **11a-d**, indicates that **12a-d** exhibit higher effectiveness or cytotoxicity against **MCF-7** than **11a-d**, as observed in **Table 1**. In case of **HepG2** human cancer cell line, the conjugates **12a-d** having the neocryptolepine core carrying at C-5 of the rhodanine ring showed the best activity with the exception of **11a**, which showed stronger activity than its regio-isomer **12a**. Conjugate **12a**, which has a phenoxy group bearing a neocryptolepine core at position C-5 of the rhodanine ring, is more active than its regio-isomer **11a** against the **A549** cancer cell line, as shown in **Table 1**. It is notable that the anticancer activity of both conjugate **12b** and its regio-isomer **11b** is identical. Notably **12c** and **12d** containing 11-phenoxy neocryptolepine at position C-5 of rhodanine ring have more antiproliferative effect comparing to their regio isomer **11c** and **11d** according to their IC_{50} values as mentioned in **Tables** 1and **6**.

Table 6: comparison between the anticancer activity the synthesized 11a-d and 12a-d against the four tested cancer cell lines

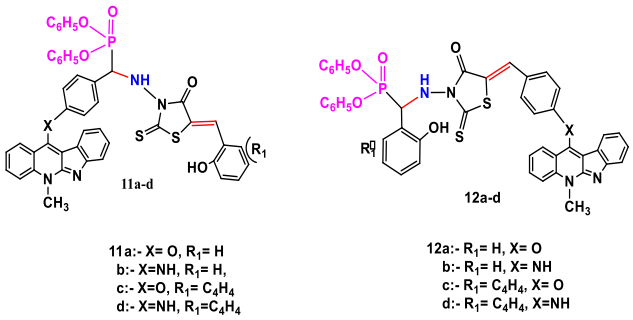

Cancer Cell Line	Conjugate (IC_{50} µM)	
HCT-116	11a (17.7)	12a (0.1)
	11b (7.5)	12b (3.7)
	11c (23.4)	12c (14.3)
	11d (5.5)	12d (15.6)
MCF-7	11a (14.1)	12a (7.4)
	11b (24.1)	12b (11.1)
	11c (20.7)	12c (17.7)
	11d (22.9)	12d (18.2)
HepG-2	11a (23.3)	12a (27.5)
	11b (26.8)	12b (24.5)
	11c (26.5)	12c (22.9)
	11d (23.9)	12d (19.4)
A549	11a (21.9)	12a (17.4)

	11b (24.9)	12b (24.5)
	11c (31.0)	12c (20.0)
	11d (22.4)	12d (19.7)

Molecular Docking

Molecular docking was demonstrated on topoisomerase-1 (TOPO-1) which was selected as a target based on the biological results that showed best performance by the conjugate **12a,** including neocryptoleine, rhodanine and aminophosphonate scaffolds against colon cancer cells HCT-116. Multiple studies specifically mention HCT116 cells in the context of TOPO-1. For instance, one study directly investigates the activity of TOPO-1 in HCT116 cells by looking at TOPO-1-DNA complexes after exposure to drugs like irinotecan - an anti-cancer medication used to treat colon cancer and small cell lung cancer- (and its active metabolite, SN38), confirming the presence and function of TOPO-1 [42]. Accordingly, a molecular docking study was performed on the synthesized compounds (**11a-d**, and **12a-d**) along with the reference drug Irinotecan on topoisomerase-1 as a target.

Topoisomerase-1 protein was downloaded from the protein data bank with pdb ID: 1K4T, the co-crystalized ligand downloaded with topoisomerase I—"2-(1-dimethylaminomethyl-2-hydroxy-8-hydroxymethyl-9-oxo-9,11-dihydro-indolizino [1,2-b]quinolin-7-yl)-2-hydroxy-butyric acid", referred to as "TGG"—defined the residues in the binding pockets [43] Asp-533, Asn-722, Lys-532, Phe-361, Gly-363, and Arg-364, as shown in **Figure 3**. TGG was stabilized by stacking interactions with the DNA, in addition to hydrogen bonds with Asp-533 and Asn-722. Residues Asp-533, Asn-722, Lys-532, and Arg-364 contributed to direct interaction with the drug. Phe-361, Arg-362, and Glu-356 were not essential for direct interaction with the drug but were stabilizing the intercalation-binding pocket. Redocking of the co-crystallized ligand was performed for validation and the recorded RMSD value was 0.94 Å. Analysis of the resulting data from docking conjugates **11a-d** and **12a-d** revealed interactions similar to those reported by TTG, with the main amino acids involved in most interactions being Lys-374, Lys-532, Arg-364, Asp-533, Arg-362, and Asn-722. The binding affinities were −10.02 to -7.32 kcal/mol with perfect fitting inside the binding site, as shown in **Table 7**. The indolo-quinoline amino phosphonate conjugate **12a** recorded the lowest IC_{50} values 0.1, 7.4, 27.5, 17.4 μM against the four tested cancer cell lines HCT-116, MCF-7, HepG2, and A549 respectively. Analyzing the recorded scores, conjugate **12a** demonstrated the best binding affinity with the least binding energy of

−10.02 kcal/mol and the amino acids residues involved in interaction with the receptor pocket were the main residues required for direct interaction with the co-crystallized ligand including Lys-532, Asp-533, and Arg-364, in addition to Phe-361, which is important for stabilizing the intercalation binding pocket, as seen in **Figure 4**. There was also hydrogen bonding at the DNA binding region at TGP11, in addition to hydrophobic bonds with DG12 and TGP 11. The docked conjugates showed high affinity that was consistent with the recorded low IC_{50} value.

Table 7: Docking results for conjugates **11a-d** and **12a-d** at the downloaded protein topoisomerase I

Compound	**Energy (kcal/mol)**	**Amino Acids (Ligand Interaction Type)**
11a	−7.32	Tyr-426(H-bond donor) Lys-425 (π-alkyl) Lys-532 (π -cation) Arg-364 (π -cation) Asp-533 (π -cation) TGP-11(π-π -T-shaped) DG-12 (π -anion)
11b	−7.79	Arg-364 (H-bond donor) DG-12 (H-bond donor) Glu-356 (H-bond acceptor) Asp-533 (H-bond acceptor) Arg-364 (π -cation) Lys-374 (π -cation)

		Asp-533 (π -anion) DG-12 (π -anion)
11c	−7.77	Arg-364 (H-bond donor) Thr-718 (H-bond donor) Arg-364 (π -cation) DG-12 (π -anion) Asp-533 (π -anion) TGP-11(π-π -T-shaped)
11d	−8.61	Tyr-426 (H-bond donor) Asn-722 (H-bond donor) Arg-364 (π -cation) Glu-356 (π -anion) Lys-374 (π -alkyl) TGP-11(π-π -T-shaped)
12a	−10.02	Arg-364 (H-bond donor) Thr-718 (H-bond donor) TGP-11(H-bond donor) Arg-364 (π -cation) Lys-532 (π -cation) Glu-356 (π -anion)

		DG-12 (π -anion) TGP-11(π-π -stacked)
12b	−9.34	Arg-364 (H-bond donor) DG-12 (H-bond donor) Asp-533 (H-bond acceptor) Arg-364 (π -cation) Asp-533 (π -anion) TGP-11 (π-π -stacked)
	−9.10	TGP-11(H-bond donor) Glu-356(H-bond acceptor) Lys-374(π -cation) Asp-533 (π -anion) DG-12 (π -anion) TGP-11 (π-π -stacked) DG-12(π-π -T-shaped)
12d	−8.70	Arg-364 (H-bond donor) Arg-364 (π -cation) Glu-356 (π -anion) Asp-533 (π -anion) DG-12 (π -anion)

		TGP-11(π-π -T-shaped)
Irinotecan	-8.43	Lys-532(H-bond donor) Arg-364 (H-bond donor) Asn-722 (H-bond donor) Glu-356(H-bond acceptor) Asp-533 (H-bond acceptor) TGP-11 (π-π -stacked)

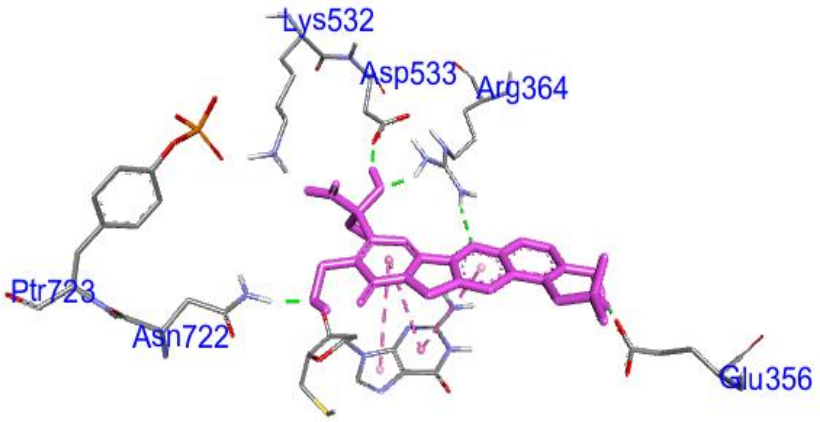

Figure 3: Site view of the co-crystallized ligand (represented as pink sticks) of topoisomerase-I showing the most important active site residues, which define the receptor pocket

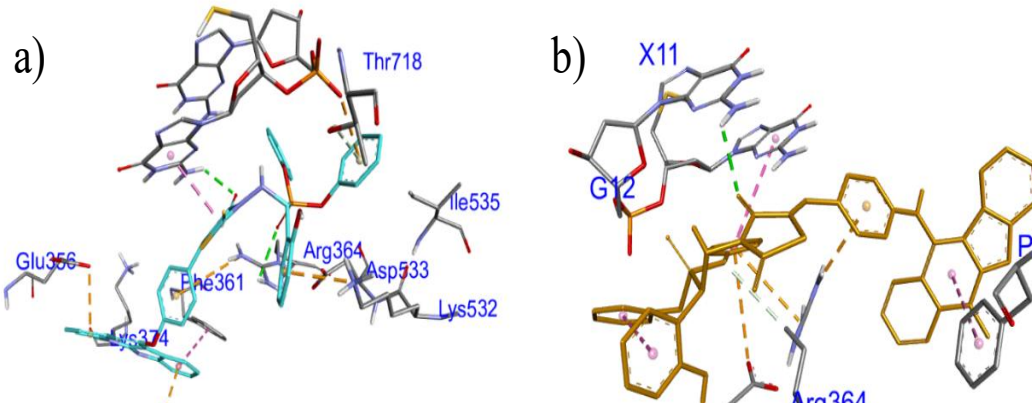

Figure 4: Docking **12 a** (represented in blue sticks) while **12b** (represented in orange sticks)in the binding cavity of topoisomerase-I

Moreover, the results indicate the involvement of Topoisomerase II (TOPO-2) in HCT116 cells. A specific HCT116 cell line, designated as topoisomerase-IIα (TOPO2A)-degron, was developed to enable the acute depletion of endogenous TOPO2A, thereby highlighting its significance in these cells. Additionally, another study examined the effects of the TOPO-2 inhibitor etoposide on HCT116 cells, which causes DNA damage and leads to G2/M cell cycle arrest, further validating the presence of TOPO2 [44].

Regarding topoisomerase-IIα (pdb ID: 5GWK), the redocking of the co-crystallized ligand was performed at the ligand binding site and showed an RMSD of 1.71 Å. Upon docking the synthesized compounds at the defined ligand site, the proposed binding mode of the docked α-aminophosphonate conjugates containing neocryptolepine-rhodanine congers **11a-d** and **12a-d** showed affinity values ranging from −8.65 to −5.85 kcal/mol. The lowest binding energies were observed in **11d** and **12a,b**. Analyzing the docking results of the best inhibitor in biological results **12a** as shown in **Figure 5**, forming interactions with the pocket residues, hydrogen bond interactions with GLY 760, SER 763, PRO 803, and ALA801, while it shows hydrophobic π-alkyl interactions with MET762, LYS 489, and PRO803, in addition to an H-bond with DC11 at the DNA hinge region, as seen in **Figure 5**. The docking results, including residues involved in the interactions as well as the types of bonding are tabulated in **Table 8**.

Table 8: Docking results for compounds 11a-d and 12a-d at the downloaded proteins topoisomerase II.

Compound	Energy (kcal/mol)	Amino acids (Ligand Interaction Type) in TOPO II
11a	−7.47	ARG 804(H-bond donor) DC 11(H-bond donor) SER 800 (H-bond acceptor) DG 13 (H-bond acceptor) DA 12(π-π -T-shaped) MET 765 (π-sulfur) In addition to π-alkyl hydrophobic interactions with DG 13, DC 14, PRO 803, MET 762)
11b	−6.27	ARG 487(H-bond donor) DA 12(H-bond donor) DA 12(π-π -stacking) DG 13(π-π -T-shaped) In addition to π-alkyl hydrophobic interactions with ARG 487, MET 762)
11c	−5.85	ARG 804(H-bond donor) DC 11(H-bond donor) DG 10 (H-bond acceptor) ARG 804(π -cation)

		DA 12(π-π -stacking) DG 13(π-π -stacking) DA12(π-π -T-shaped) In addition to π-alkyl hydrophobic interactions with DA 12, DG 13, PRO 803, MET 762)
11d	−8.65	DG 13(H-bond acceptor) SER 802(H-bond donor) DA 12(H-bond acceptor) ALA 801(H-bond acceptor) DA 12(H-bond donor) DA 12(π-π -stacking) DC 11(π-π -T-shaped) In addition to alkyl hydrophobic interactions with ILE 769, PRO 803, MET 766) and π -alkyl interactions with MET 762 and PRO 803.
12a	−8.26	GLY 760(H-bond donor) SER 763(H-bond donor) SER 763(H-bond acceptor) PRO 803(H-bond donor) ALA 801(H-bond acceptor) DC 11(H-bond donor)

		MET 766(π-sulfur) In addition to π-alkyl hydrophobic interactions with LYS 489, PRO 803, MET 762)
12b	−8.47	PRO 803(H-bond donor) DC 11(H-bond donor) DG 13(π-π -stacking) In addition to π-alkyl hydrophobic interactions with ARG 487, PRO 803, MET 762, MET 766)
12c	−7.37	DG 13(H-bond donor) GLY 488(H-bond donor) DG 10(H-bond donor) DG 10(H-bond acceptor) ARG 804(π -cation) GLU 461(π -anion) DC 11(π-π -T-shaped) DA 12(π-π -T-shaped) DC 11(π-π -T-shaped) In addition to π-alkyl hydrophobic interactions with ARG 487, DT 9, DG 10, MET 762)
12d	−8.17	GLY 760(H-bond donor) DC 11(H-bond acceptor)

	DG 13(π-π -T-shaped)
	In addition to π-alkyl hydrophobic interactions with PRO 803, MET 762)

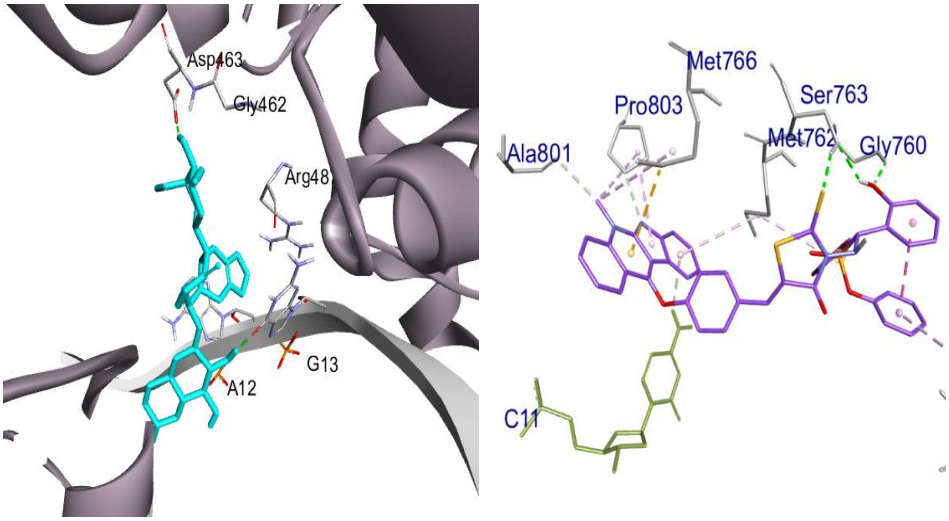

Figure 5: The co-crystallized ligand of the downloaded protein pdb ID; a 5GWK (in blue sticks)-defining receptor pocket, compound 12a (represented in purple sticks) and the amino-acids residues interacting in the binding pocket of topo-2

Conclusion

Novel conjugates of neocryptolepine, rhodanine and α –aminophosphonate 11a-d and 12a-d were designed, synthesized, and characterized. The antiproliferative activity against four types of human cancer cell lines confirmed that the synthesized conjugates have more potency than the reference drug, doxorubicin especially 12a against HCT-116, MCF-7, HepG2 and A549. Furthermore, most of the synthesized conjugates have low toxicity towards RPE-1 cell line. In addition, 12a recorded high binding affinity against topoisomerase-1 and II in molecular docking studies, which is consistent with the biological results in particular against colon cancer cells.

Experimental

All NMR analyses were conducted using DMSO-d_6 as a solvent, Jeol 500 MHz, and 125 MHz for ^{1}H NMR and ^{13}C NMR, respectively. Using a Shimadzu IR 435 spectrophotometer, FTIR spectroscopy was conducted. EI-MS spectrometry with an ISQ single quadrupole thermoscientific

trace 1310 gas chromatograph in Electron Impact mode was performed at the regional center for mycology and biotechnology, Azhar University, Cairo, Egypt. Melting points were recorded using a melting point apparatus from Stuart Scientific. Raw materials and solvents were purchased and used without further purification. It is worth mentioning that the previously reported method [22] for the preparation of **3a.** Additionally, Schiff bases **8a** and **8b** was prepared as outlined in the reported literature [35, 36].

Chemistry

Procedure for Synthesis of 11- formyl neocryptolepine (3b)

To (1 g, 3.75 mmol) of 11-chloroneocryptolpine **1**, add (0.92 g, 7.50 mmol) of 4-aminobenzaldehyde **2b** and (1.04 g, 7.50 mmol) of anhydrous potassium carbonate in DMF (5 mL), then reflux for 24 hours until the complete consumption of the reactant. The reaction mixture was refluxed and monitored with TLC until. The mixture was poured into cold water, then further cooled, filtered and dried. Further recrystallization was carried out using ethanol to get yield **3**.

4-((5-methyl-5H-indolo[2,3-b]quinolin-11-yl)amino)benzaldehyde (3b)

Yellow solid, Yield: (0.90 g, 68%), melting point: 196.2-197.6 °C, **FTIR** (KBr) cm^{-1}: 3410(NH), 3047 (=CH), 2924 (CH), 1696 (C=O), 1612 ($C=C_{Ar}$). **^{1}H NMR** δ: 4.27(s, 3H, CH_3), 7.38-7.93(m, 13H, CH_{Ar}), 9.30(s, 1H, CHO), **^{13}C NMR** δ: 34.42 (*N*-CH_3); (C Aromatic):115.94, 116.06, 119.03, 120.92, 121.72, 125.59, 126.84, 130.31, 138.41, 141.22, 157.47 (C=N indole), 190.82 (CHO). **EI-MS**: calcd. for ($C_{23}H_{17}N_3O$) m/z: 351.41 $[M]^+$; found 353.22.

General procedure for synthesis of Schiff bases (5 and 8):

In a solution of *N*-aminorhodanine **4** (0.44 g, 3 mmol) dissolved in 5 mL of ethanol, (3 mmol) of aldehydes **3** (0.37g) or **6** (0.51 g) and a few droplets of glacial acetic acid were added to the rection mixture, which was then refluxed. TLC was used to monitor the progression of the reaction until all reactants were consumed after 2 to 3 hours. The reaction mixture was cooled and poured into cold water, after which it was filtered, collected and dried to produce **5** or **8** with satisfactory yields.

*((4-((5-methyl-5H-indolo[2,3-b]quinolin-11-yl)oxy)benzylidene)amino)-2-thioxothiazolidin-4-one (**5a**)*

Yellow solid, yield: (0.90 g, 62 %), m.p: 168.4-169.1 °C, **FTIR** (KBr) cm^{-1} υ: 3062 (=CH), 2970 (CH), 1712 (C=O), 1612 (C=C, Ar), 1581 (C=N), 1211 (C=S). **^{1}H NMR** δ: 3.99(s, 3H, CH_3), 5.94 (s, 2H, CH_2), 7.18-8.37 (m, 12H, CH_{Ar}), 8.39 (s, 1H, C<u>H</u>=N), 12.25(br.s, 1H, tautomer OH). **^{13}C NMR** δ: 33.19 (*N*-CH_3), 49.07 (S-CH_2); (C aromatic) 102.86, 111.38, 115.75, 115.75, 116.18, 117.31,120.68, 121.61, 122.13, 122.77, 123.33, 124.43, 125.02, 125.46, 126.25, 129.86, 131.67, 133.91, 135.36, 139.59 (C=N, Schiff base), 147.49 (C=N, indole ring), 172.09 (C=O), 191.37 (C=S). **EI-MS**: calcd. for ($C_{26}H_{18}N_4O_2S_2$) m/z: 482.58 $[M]^+$; found 484.07.

3-((4-((5-methyl-5H-indolo[2,3-b]quinolin-11yl)amino)benzylidene)amino)-2-thioxothiazo-lidin-4-one (5b)

Brown solid, yield: (0.87 g, 60 %), m.p: 200.6-201.3°C, **FTIR** (KBr) cm^{-1} υ: 3425 (OH+NH overlapped), 3093 (=CH), 2970 (CH), 1735(C=O), 1612 (C=C $_{Ar}$), 1581 (C=N), 1211 (C=S) **^{1}H NMR** δ: 3.98(s, 3H, CH_3), 5.71 (s, 2H, CH_2), 7.23 - 8.39 (m, 12H, CH_{Ar}), 8.48 (s, 1H, C<u>H</u>=N), 12.09 (br.s, 1H, NH). **^{13}C NMR** δ: 33.73 (*N*-CH_3), 45.24(S-CH_2), 102.75, 111.26, 115.66, 116.95, 120.59, 121.63, 122.12, 123.26, 124.08, 124.52, 125.14, 126.23, 127.59, 128.06, 131.64, 135.19, 139.64 (C=N, Schiff base), 147.37 (C=N, indole ring), 172.01(C=O), 199.53 (C=S). **EI-MS**: calcd. for ($C_{26}H_{19}N_5OS_2$) m/z: 481.59$[M]^+$; found 483.85.

General procedure for synthesis of neocryptolepine – rhodanine congers 7a-d and 9a-d

Sodium acetate (0.10 g, 1.03 mmol) was added to the mixture of Schiff bases **5** or **8** (0.20 g, 0.41 mmol) and aldehydes **3**, **6** (0.16 g, 0.45 mmol) dissolved in ethanol and the reaction mixture was refluxed for 3 to 4 hours and it was monitored by TLC till the completion of the reaction. The reaction mixture was then poured into freezing water, filtered, collected, and dried to produce high yields of **7a-d** or **9a-**d after recrystallization from ethanol as illustrated [35, 36].

*5-((Z)-2-hydroxybenzylidene)-3-((Z)4-((5-methyl-5H-indolo[2,3-b]quinolin-11-yl)oxy)benzylidene)amino)-2-thioxothiazolidin-4-one (**7a**)*

Brown solid, yield: (0.13 g, 52 %), m.p: 118.7-119.4°C, **FTIR** (KBr) cm^{-1} υ: 3441(OH+NH overlapped), 3055(=CH), 2970(CH), 1705 (C=O), 1612 (C=C_{Ar}), 1573 (C=N), 1211 (C=S) .**^{1}H NMR** δ: 3.98(s, 3H, CH_3), 7.22-7.82 (m,12H, CH_{Ar}), 7.94 (s,1H,C<u>H</u>=C), 8.20 (d, 2H, CH_{Ar}, *J* = 8 MHz) , 8.39 (s, 2H, CH_{Ar}), 9.00 (s, 1H, C<u>H</u>=N), 12.08 (s,1H,OH). **^{13}C NMR** δ: 33.71(*N*-CH_3), (C aromatic) 111.24, 115.60, 116.22, 120.59, 122.07, 122.77, 123.22, 124.52, 125.14, 125.49, 126.21, 129.84, 131.40, 131.58, 133.66, 135.18, 135.30, 137.09, 139.61, 143.03 (C=C exocyclic),

147.34, 159.11(C=N Schiff base), 163.24 (C=N indole), 171.99, 183.53 (C=O), 194.45 (C=S). **EI-MS**: calcd. for ($C_{33}H_{22}N_4O_3S_2$) m/z: 586.68[M]$^+$; found 587.44.

*5-((Z)-2-hydroxybenzylidene)-3-((Z)4-((5-methyl-5H-indolo[2,3-b]quinolin-11-yl)amino)benzylidene)amino)-2-thioxothiazolidin-4-one (7**b**)*

Brown solid, yield (0.12 g, 50%), m.p: 226.4-227.2°C, **FTIR** (KBr) cm^{-1} υ: 3425 (OH+NH overlapped), 3047 (=CH), 2978 (CH), 1712 (C=O), 1612 (C=C$_{Ar}$), 1581(C=N), 1211(C=S). **^{1}H NMR** δ: 3.98(s, 3H, CH_3), 7.21-7.86 (m,12H, CH$_{Ar}$), 8.12 (s,1H, C<u>H</u>=C), 8.20 (d, 2H, CH$_{Ar}$, *J*=8 Hz), 8.39 (d, 2H, CH$_{Ar}$, *J*=8 Hz), 8.93 (s,1H, C<u>H</u>=N), 10.79 (s,1H, NH), 12.10 (s,1H, OH). **^{13}C NMR** δ: 33.75 (*N*-CH_3), (C aromatic) 102.77, 111.28, 115.70, 119.27, 120.36, 120.63, 121.67, 122.16, 123.29, 123.97, 124.54, 129.83, 131.68, 135.21, 139.66 (C=C exocyclic), 147.40 (C=N Schiff base, indole), 172.04 (C=O), 195.19 (C=S). **EI-MS**: calcd. for ($C_{33}H_{23}N_5O_2S_2$) m/z: 585.70 [M]$^+$; found 587.72.

*(Z)-5-((3-hydroxynaphthalen-2-yl)methylene)-3-(Z)4-((5-methyl-5H-indolo[2,3-b]quinolin-11-yl)oxy) benzylidene)amino)-2-thioxothia- zolidin-4-one (7**c**)*

Yellow solid, yield (0.13 g, 48 %), m.p: 188.5-189.8°C, **FTIR** (KBr) cm^{-1} υ: 3417 (OH+NH overlapped), 3055 (=CH), 2947 (CH), 1735 (C=O), 1612 (C=C$_{Ar}$), 1581 (C=N), 1203 (C=S). **^{1}H NMR** δ: 3.98 (s, 3H, CH_3), 7.22 -7.90 (m,14H, CH$_{Ar}$), 8.04 (s,1H, C<u>H</u>=C), 8.18 (d, 2H, CH$_{Ar}$, *J*=8 Hz), 8.39 (s, 2H, CH$_{Ar}$), 8.63 (s,1H, C<u>H</u>=N), 12.08 (s,1H, OH). **^{13}C NMR** δ: 33.72 (*N*-CH_3), (C aromatic) 102.70, 111.32, 115.73, 118.24, 120.36, 120.72, 121.64, 122.36, 123.29, 124.14, 124.62, 125.36, 126.54, 129.51, 131.42, 135.28, 139.45(C=C exocyclic) 147.31(C=N Schiff base, indole), 172.16 (C=O), 192.79 (C=S). **EI-MS**: calcd. for ($C_{37}H_{24}N_4O_3S_2$) m/z: 636.74 [M]$^+$; found 638.12.

*(Z)-5-((3-hydroxynaphthalen-2-yl)methylene)-3-((Z)4-((5-methyl-5H-indolo[2,3-b]quinolin-11-yl)amino) benzylidene)amino)-2-thioxothia- zolidin-4-one (7**d**)*

Brown solid, yield (0.12 g, 45 %), m.p: 190-193°C, **FTIR** (KBr) cm^{-1} υ: 3448 (OH+NH overlapped), 3055 (=CH,), 2970 (CH), 1705 (C=O), 1620 (C=C$_{Ar}$), 1581 (C=N), 1141 (C=S). **^{1}H NMR** δ: 3.96 (s, 3H, CH_3), 7.22-7.80 (m, 14H, CH$_{Ar}$), 7.96 (s, 1H, C<u>H</u>=C), 8.20 (d, 2H, CH$_{Ar}$, *J* = 8 Hz), 8.39(d, 2H, CH$_{Ar}$, *J*= 8 Hz), 9.00 (s,1H,C<u>H</u>=N), 12.09 (s, 2H, OH+NH overlapped).**^{13}C NMR** δ: 33.75 (*N*-CH_3), (C aromatic) 102.76, 111.27, 115.70, 119.41, 120.62, 121.66, 122.15, 122.63, 123.28, 124.56, 126.26, 129.28, 129.73, 131.67, 135.20, 138.85, 139.68 (C=C exocyclic),

147.40 (C=N Schiff base, indole), 172.02 (C=O), 193.30(C=S). **EI-MS**: calcd. for ($C_{37}H_{25}N_5O_2S_2$) m/z: 635.76 $[M]^+$; found 637.65.

*3-((Z)-2-hydroxybenzylidene)amino)-5-((Z)-4-((5-methyl-5H-indolo[2,3-b]quinolin-11-yl)oxy)benzylidene)-2-thioxothiazolidin-4-one (**9a**)*

Brown solid, yield (0.60 g, 51 %), m.p: 150-152°C, **FTIR** (KBr) cm^{-1} υ: 3417(OH+NH overlapped), 3062(=CH), 2970 (CH), 1712 (C=O), 1612 ($C=C_{Ar}$), 1581(C=N), 1157 (C=S. **^{1}H NMR** δ: 3.96(s, 3H, CH_3). 7.22- 7.80 (m, 12H, CH_{Ar}), 7.93(s, 1H, C<u>H</u>=C), 8.19 (d, 2H, CH_{Ar}, *J* = 8 Hz), 8.39 (d, 2H, CH_{Ar}, *J* = 8 Hz), 8.98 (s, 1H, C<u>H</u>=N), 12.06 (m, 1H, OH). **^{13}C NMR** δ: 34.66 (*N*-CH_3), (C aromatic) 102.76, 111.24, 115.60, 116.22, 119.27, 120.59, 121.60, 121.80, 122.07, 122.77, 123.22, 123.41, 124.52, 125.14, 125.49, 126.21, 129.84, 131.40, 135.18, 139.61(C=C exocyclic), 159.11(C=N Schiff base, indole), 171.99 (C=O), 183.53(C=S). **EI-MS**: calcd. for ($C_{33}H_{22}N_4O_3S_2$) m/z: 586.68 $[M]^+$; found 588.17.

*3-((Z)-2-hydroxybenzylidene)amino)-5-((Z)-4-((5-methyl-5H-indolo[2,3-b]quinolin-11-yl)amino)benzylidene)-2-thioxothiazolidin-4-one (**9b**)*

Brown solid, yield (0.57 g, 48%), m.p: 223-226°C, **FTIR** (KBr) cm^{-1} υ: 3402 (OH+NH overlapped), 3047(=CH), 2978(CH), 1705(C=O), 1620 ($C=C_{Ar}$), 1581(C=N), 1157 (C=S). **^{1}H-NMR** δ: 3.98 (s, 3H, CH_3), 7.23- 7.78 (m, 12H, CH_{Ar}), 7.94 (s, 1H, C<u>H</u>=C), 8.18 (d, 2H, CH_{Ar}, *J* = 8 Hz), 8.37 (d, 2H, CH_{Ar}, *J* = 8 Hz), 9.00 (s, 1H, C<u>H</u>=N), 10.74 (s,1H, NH), 12.07 (m, 1H, OH) **^{13}C-NMR** δ: 33.75 (*N*-CH_3), (C aromatic) 102.76, 111.28, 115.69, 116.63, 120.61, 121.06, 121.65, 122.14, 123.27, 124.05, 125.18, 126.25, 127.51, 127.84, 131.66, 135.21(C=C exocyclic), 147.39(C=N Schiff base, indole), 172.02 (C=O),196.64 (C=S). **EI-MS**: calcd. for ($C_{33}H_{23}N_5O_2S_2$) m/z: 585.70 $[M]^+$; found 587.46.

*3-((Z)2-hydroxynaphthalen-1-yl)methylene)amino)-5-((Z)-4-((5-methyl-5H-indolo[2,3-b]quinolin-11-yl)oxy)benzylidene)-2-thioxo thiazolidin-4-one (**9c**)*

Yellow solid, yield: (0.69 g, 54 %), m.p: 128.4-129.6°C, **FTIR** (KBr) cm^{-1} υ:3417(OH+NH overlapped), 3055 (=CH), 2970 (CH), 1712 (C=O), 1612 ($C=C_{Ar}$), 1581(C=N), 1157 (C=S). **^{1}H NMR** δ: 3.96 (s, 3H, CH_3), 7.20-7.89 (m, 14H, CH_{Ar}), 8.01 (s, 1H, C<u>H</u>=C), 8.19 (d, 2H, CH_{Ar}, *J* = 8 Hz), 8.38 (d, 2H, CH_{Ar}, *J* = 8 Hz), 8.64 (s, 1H, C<u>H</u>=N), 12.06 (s, 1H, OH). **^{13}C NMR** δ: 33.78 (*N*-CH_3), (C aromatic) 111.28, 115.63, 116.38, 120.69, 122.27, 122.85, 123.18, 124.49, 125.14, 125.32, 125.53, 126.44, 128.73, 131.42, 131.66, 133.78, 135.07, 135.35, 138.17, 139.63,143.13

(C=C exocyclic), 147.25 (C=N Schiff base), 159.19 (C=N indole), 163.30, 171.85, 183.63(C=O),194.48 (C=S). **EI-MS**: calcd. for ($C_{37}H_{24}N_4O_3S_2$) m/z: 636.74[M]$^+$; found 638.87**.**

3-((Z)-(2-hydroxynaphthalen-1-yl)methylene)amino)-5-((Z)-4-((5-methyl-5H-indolo[2,3-b]quinolin-11-yl)amino)benzylidene)-2-thioxothiazolidin-4-one ***(9d)***

Yellow solid, yield (0.63 g, 49 %), m.p: 220-222°C, **FTIR** (KBr) cm^{-1} υ: 3464 (OH+NH overlapped), 3309 (NH), 3047 (=CH), 2931(CH), 1697 (C=O), 1604 (C=C$_{Ar}$), 1566 (C=N), 1226 (C=S*)*. **^{1}H NMR** δ: 3.98(s, 3H, CH_3), 7.19- 7.89 (m, 14H, CH_{Ar}), 8.08 (s, 1H, C<u>H</u>=C), 8.20 (d, 2H, CH_{Ar}, *J* = 8 Hz), 8.39 (d, 2H, CH_{Ar}, *J* = 8 Hz), 8.65 (s, 1H, C<u>H</u>=N), 11.26 (br.s, 1H, NH), 12.07 (s, 1H, OH). **^{13}C NMR** δ: 33.62 (*N*-CH_3), (C aromatic) 111.27, 115.72, 116.34, 120.68, 122.12, 122.65, 123.34, 124.45, 125.19, 125.20, 125.65, 127.23, 129.74, 131.35, 131.67, 132.54, 135.14, 135.35, 137.11, 139.56, 143.04 (C=C exocyclic), 146.24(C=N Schiff base), 158.27(C=N indole), 163.23, 171.94, 183.63 (C=O), 193.68 (C=S). **EI-MS**: calcd. for ($C_{37}H_{25}N_5O_2S_2$) m/z: 635.76 [M]$^+$; found 636.54.

General procedure for synthesis of neocrytolepine-α-aminophosphonate conjugates 11a-d and 12a-d

To (1.17 g, 5mmol) of diphenyl phosphite **8**, (5mmol) of neocryptolepine-rhodanine congers **7** (2.92 g) or **9** (3.18g) dissolved in 5mL of methanol was added and the mixture was refluxed for 3 to 4 hours. Good yields of products **11a-d** or **12a-d** were obtained by recrystallizing the precipitate from ethanol.

Diphenyl(Z)-(((5-(2-hydroxybenzylidene)-4-oxo-2-thioxothiazolidin-3-yl)amino)(4-((5-methyl-5H-indolo[2,3-b]quinolin-11-yl)oxy)phenyl)methyl) phosphonate ***(11a)***

FTIR (KBr) cm^{-1} υ: 3410 (OH+NH overlap), 3032 (=CH), 2954 (CH), 1697 (C=O), 1612 (C=C$_{Ar}$), 1589 (C=N), 1249 (P=O), 1188 (C=S). **^{1}H NMR** δ 3.99 (s, 3H, CH_3), 6.74 (d, 1H, C<u>H</u>-P, *J*=8 Hz), 7.23-7.80 (m, 22H, CH_{Ar}), 7.94 (s, 1H, C<u>H</u>=C), 8.19 (d, 2H, CH_{Ar}, *J* = 8 Hz), 8.40 (d, 2H, CH_{Ar}, *J* = 8 Hz), 12.13 (s,1H, NH), 12.45 (s, 1H, OH). **^{13}C NMR** δ: 33.59 (*N*-CH_3), 56.28 (CH-P), (C aromatic) 102.65, 112.28, 114.45, 115.83, 119.78, 121.74, 122.19, 123.32, 124.42, 125.27, 126.32, 128.61, 129.45, 129.56, 131.68, 135.22, 139.54, 147.61(C=C exocyclic), 158.26 (C=N indole), 172.03 (C=O), 193.41 (C=S). **EI-MS**: calcd. for ($C_{45}H_{33}N_4O_6PS_2$) m/z: 820.87 [M]$^+$; found 821.40.

*Diphenyl(Z)-(((5-(2-hydroxybenzylidene)-4-oxo-2-thioxothiazolidin-3-yl)amino)(4-((5-methyl-5H-indolo[2,3-b]quinolin-11yl)amino)phenyl)methyl) phosphonate (**11b**)*

Brown solid, yield (0.43 g, 53 %), m.p: 226-228 °C, **FTIR** (KBr) cm^{-1} υ: 3417 (OH+NH overlapped), 3055 (=CH), 2939 (CH), 1681 (C=O), 1612 (C=C_{Ar}), 1581(C=N), 1234 (P=O), 1157 (C=S). **^{1}H-NMR** δ: 3.98 (s, 3H, CH_3), 6.74 (d, 1H, C<u>H</u>-P, *J*=8 Hz), 7.22-7.79 (m, 22H, CH_{Ar}), 7.97 (s, 1H, C<u>H</u>=C), 8.20 (d, 2H, CH_{Ar}, *J* = 8 Hz), 8.39 (d, 2H, CH_{Ar}, *J* = 8 Hz), 10.80 (s,1H,NH), 12.08 (s,1H,OH). **^{13}C-NMR** δ: 34.71 (*N*-CH_3), 55.42 (CH-P), (C aromatic) 102.44, 112.34, 115.62, 120.53, 121.66, 122.24, 123.36, 124.44, 125.16, 126.38, 128.25, 129.65, 130.43, 131.59, 132.26, 138.67(C=C exocyclic), 146.49(C=N indole), 172.10 (C=O), 193.31 (C=S). **EI-MS**: calcd. for ($C_{45}H_{34}N_5O_5PS_2$) m/z: 819.89 $[M]^+$; found 820.61**.**

*Diphenyl(Z)-(((5-((3-hydroxynaphthalen-2-yl)methylene)-4-oxo-2-thioxothiazolidin-3-yl)amino)(4-((5-methyl-5H-indolo[2,3-b]quinolin-11-yl)oxy)phenyl) methyl)phosphonate (**11c**)*

Yellow solid, yield (0.64 g, 53 %), **FT IR** (KBr) cm^{-1} υ: 3425 (OH+NH overlapped), 3124 (=CH), 2985 (CH), 1674 (C=O), 1643 (C=C_{Ar}), 1519 (C=N), 1342 (P=O) 1157 (C=S). **^{1}H NMR** δ: 3.96 (s, 3H, CH_3), 6.73 (d, 1H, C<u>H</u>-P, *J*=8Hz), 7.19-7.76 (m, 24H, CH_{Ar}), 7.79 (s, 1H, C<u>H</u>=C), 8.19 (m, 2H, CH_{Ar}), 8.37(d, 2H, CH_{Ar}, *J* = 8 Hz),12.07 (s,2H, OH+NH). **^{13}C NMR** δ: 33.75 (*N*-CH_3), 57.26 (CH-P), 58.35 (CH-P), (C aromatic) 102.77, 111.28, 115.65, 115.96, 120.60, 121.62, 122.11, 123.25, 124.54, 125.17, 126.24, 128.67, 129.36, 129.66, 131.62, 135.22, 139.65, 147.38 (C=C exocyclic), 158.21 (C=N indole), 172.02 (C=O), 183.46 (C=S). **EI-MS**: calcd. for($C_{49}H_{35}N_4O_6PS_2$) m/z: 870.93 $[M]^+$; found 872.13.

*Diphenyl(Z)-(((5-((2-hydroxynaphthalene-1-yl)methylene)-4-oxo-2-thioxothiazolidin-3-yl)amino)(4-((5-methyl-5H-indolo[2,3-b]quinolin-11-yl)amino)phenyl)methyl)phosphonate (**11d**)*

brown solid, yield (0.63 g, 54 %), **FTIR** (KBr) cm^{-1} υ: 3425 (OH+NH overlapped), 3062(=CH), 2954(CH), 1697 (C=O), 1612 (C=C_{Ar}), 1581 (C=N), 1396 (P=O), 1141 (C=S). **^{1}H NMR** δ: 3.98 (s, 3H, CH_3), 6.73 (d, 1H, C<u>H</u>-P, *J*=8Hz), 7.23-7.77 (m, 24H, CH_{Ar}), 7.79 (s, 1H, C<u>H</u>=C), 8.18 (d, 2H, CH_{Ar}, *J* = 8 Hz), 8.39 (d, 2H, CH_{Ar}, *J* = 8 Hz), 12.09 (s,2H, OH+NH).**^{13}C NMR** δ: 33.75 (*N*-CH_3),, 53.47 (CH-P), (C aromatic) 111.28, 115.71, 120.62, 121.66, 122.16, 123.28, 124.55, 125.18, 126.26, 129.31, 129.78, 130.63, 131.68, 135.21, 139.68 (C=C exocyclic), 147.40 (C=N indole), 172.03(C=O), 192.25 (C=S). **EI-MS**: calcd. for ($C_{49}H_{36}N_5O_5PS_2$) m/z: 869.95 $[M]^+$; found 869.16.

*Diphenyl-((2-hydroxyphenyl)((-5-(Z)4-((5-methyl-5H-indolo[2,3-b]quinolin-11-yl)oxy)benzylidene)-4-oxo-2-thioxothiazolidin-3-yl)amino)methyl)phosphonate (**12a**)*

Yellow solid, yield (0.44 g, 54 %), m.p: 125.4-126.6°C, **FTIR** (KBr) cm^{-1} υ: 3441 (OH+NH overlapped), 3062 (=CH), 2978 (CH), 1705 (C=O), 1612 (C=C $_{Ar}$), 1573 (C=N), 1242 (P=O), 1157 (C=S). **^{1}H NMR** δ: 3.96 (s, 3H, CH_3), 6.74 (d, 1H, C<u>H</u>-P, *J*= 8 Hz), 7.20-7.79 (m, 22 H, CH_{Ar}), 7.90 (s,1H, CH=C), 8.19 (d, 2H, CH_{Ar}, *J* = 8 Hz), 8.38 (d,2H, CH_{Ar}, *J* = 8 Hz), 12.05 (s, 1H, NH), 12.39 (s, 1H, OH). **^{13}C NMR** δ: 34.67 (*N*-CH_3), 58.15 (CH-P), 58.80 (CH-P), (C aromatic)102.75, 111.25, 115.60, 116.21, 117.54, 119.24, 120.58, 121.60, 121.80, 122.07, 122.77, 123.22, 123.40, 124.52, 125.13, 125.49, 126.20, 129.83, 131.39, 131.57, 135.18, 135.29, 137.09, 139.60, 143.02 (C=C exocyclic),147.33 (C=N indole), 172.01(C=O),183.49 (C=S). **EI-MS**: calcd. for ($C_{45}H_{33}N_4O_6PS_2$) m/z: 820.87 $[M]^+$; found 822.82.

*Diphenyl-((2-hydroxyphenyl)((5-(Z)(4-((5-methyl-5H-indolo[2,3-b]quinolin-11-yl)amino)benzylidene)-4-oxo-2-thioxothiazolidin-3-yl)amino)methyl)phosphonate (**12b**)*

Brown solid, yield (0.45 g, 54 %), m.p: 198.4-199.8°C, **FTIR** (KBr) cm^{-1} υ: 3425 (OH+NH overlapped), 3062 (=CH), 2931 (CH), 1735 (C=O), 1620 (C=C_{Ar}), 1589 (C=N), 1242 (P=O), 1157 (C=S) **^{1}H NMR** δ: 3.97 (s, 3H, CH_3), 6.73 (d, 1H, C<u>H</u>-P, *J*=8Hz), 7.14-7.86 (m, 22H, CH_{Ar}), 8.00 (s,1H,C<u>H</u>=C), 8.18 (d, 2H, CH_{Ar}, *J* = 8 Hz), 8.39 (d, 2H, CH_{Ar}, *J*=8 Hz), 10.12 (br.s, 1H, NH), 11.25 (br.s, 1H, NH), 12.09 (s,1H,OH).**^{13}C NMR** δ: 33.74 (*N*-CH_3), 66.61(CH-P), 67.47(CH-P), (C aromatic) 102.77, 111.22, 115.56, 116.55, 120.61, 121.64, 122.21, 123.27, 126.24, 128.42, 129.88, 131.63, 135.20, 137.73, 139.64, 142.98, 147.37(C=C exocyclic), 152.38, 158.99 (C=N indole), 172.02(C=O), 185.30 (C=S). **EI-MS**: calcd. for ($C_{45}H_{34}N_5O_5PS_2$) m/z: 819.89 $[M]^+$; found 821.90.

Diphenyl-((2-hydroxynaphthalen-1-yl)((-5-(Z)(4-((5-methyl-5H-indolo[2,3-b]quinolin-11-yl)oxy)benzylidene)-4-oxo-2-thioxothiazolidin-3-yl)amino)methyl)phosphonate (12c)

Brown solid, yield (0.47 g, 54 %), m.p: 108.1-109.8 °C, **FTIR** (KBr) cm^{-1} υ: 3417 (OH+NH overlapped), 3055(=CH), 2970 (CH), 1712 (C=O), 1612 (C=C_{Ar}), 1581(C=N), 1249 (P=O), 1157 (C=S). **^{1}H NMR** δ: 4.04 (s, 3H, CH_3), 6.74 (d, 1H, C<u>H</u>-P, *J*=8Hz), 7.14-7.97 (m, 26H, CH_{Ar}), 8.04 (s, 1H, CH=C), 8.18 (d, 2H, CH_{Ar}, *J* = 8 Hz), 8.44 (d, 2H, CH_{Ar}, *J* = 8 Hz), 11.99 (br.s, 1H, NH), 12.52 (s, 1H, OH). **^{13}C NMR** δ: 33.74 (*N*-CH_3), 54.45 (CH-P), (C aromatic) 111.26, 115.67, 119.34, 120.59, 121.63, 122.12, 123.24, 124.54, 125.07, 125.17, 126.24, 127.83, 129.22, 129.94, 131.63, 135.20, 139.66, 147.37(C=C exocyclic), 153.23, 155.36 (C=N indole), 172.00 (C=O), 193.45(C=S). **EI-MS**: calcd. for ($C_{49}H_{35}N_4O_6PS_2$) m/z: 872.95 $[M]^+$; found 873.63.

*Diphenyl-((2-hydroxynaphthalen-1-yl)((-5--(Z)(4-((5-methyl-5H-indolo[2,3-b]quinolin-11-yl)amino)benzylidene)-4-oxo-2-thioxothiazolidin-3-yl)amino)methyl)phosphonate (**12d**)*

Brown solid, yield (0.43 g 54 %), m.p:103.2-105.6°C, **FTIR** (KBr) cm^{-1} υ: 3404 (OH+NH overlapped), 3055 (=CH), 2947 (CH), 1697 (C=O), 1612 (C=C $_{Ar}$), 1573(C=N), 1242 (P=O), 1157 (C=S). **^{1}H NMR** δ: 3.98 (s, 3H, CH_3), 6.73 (d, 1H, C<u>H</u>-P, *J*=8Hz), 7.20-7.87 (m, 26H, CH_{Ar}), 7.95 (d, 2H, CH_{Ar}, *J* = 8 Hz), 8.37 (d, 2H, CH_{Ar}, *J* = 8 Hz), 12.10 (br.s, 1H, NH), 12.89 (s, 1H, OH). **^{13}C NMR** δ: 33.65 (*N*-CH_3), 57.52 (CH-P), 58.31(CH-P), 111.26, 115.49, 119.10, 119.61, 120.55, 121.71, 122.91, 123.95, 125.10, 126.18, 126.35, 127.81, 128.36, 129.49, 129.64, 131.72, 133.75, 135.24, 139.53, 147.30(C=C exocyclic), 154.84, 156.13 (C=N indole), 168.63 (C=O), 188.59 (C=S). **EI-MS**: calcd. for ($C_{49}H_{36}N_5O_5PS_2$) m/z: 869.95 $[M]^+$; found 871.44.

Antiproliferative activity

Human colorectal carcinoma (HCT 116, ATCC® CCL-247™), human breast adenocarcinoma (MCF-7, ATCC® HTB-22™), human hepatocellular carcinoma (HepG2, ATCC® HB-8065™), human lung carcinoma (A549, ATCC® CCL-185™) and normal human retinal pigment epithelial (RPE-1, ATCC® CRL-4000™) cell lines were supplied from the American Type Culture Collection (ATCC, Rockville, MD). These cell lines were grown in DMEM medium supplemented with 10% heat-inactivated fetal bovine serum (FBS), 100 U/mL penicillin, and 100 U/mL streptomycin. The cells were cultured in a 37°C, 5% CO_2 atmosphere with humidity.

MTT cytotoxicity assay

The cytotoxicity of HCT-116, MCF-7, HepG2, and A549 cancer cell lines were evaluated using the 3-[4,5-dimethyl-2-thiazolyl]-2,5-diphenyl-2H-tetrazolium bromide (MTT) assay as described in literature [39, 45-47]. This assay relies on the reduction of the tetrazolium salt by mitochondrial dehydrogenases in viable cells. Cells were seeded in a 96-well sterile microplate (2 x 10^4 cells/well) and cultured in a serum-free medium with increasing doses of each compound or Doxorubicin (positive control) in DMSO for 48 hours at 37 degrees Celsius before the MTT assay. After carefully draining the medium, then 40 µL of MTT (2.5 mg/mL) was added to each well and incubated for another 4 hours. Exactly 200 µL of DMSO was enough to dissolve the purple formazan crystals. For this experiment, the Spectra Max Paradigm Multi-Mode microplate reader was used to determine the absorbance at 570 nm. To determine relative cell viability, the mean percentage of live cells was compared to the untreated control cells.

Statistical Analysis

Each test was repeated three times, on three separate occasions. Then the average standard error mean of the numbers was calculated using (IBM Corp., Armonk, NY, USA) SPSS Inc. where probit analysis was used to calculate IC_{50} values.

Molecular docking

Molecular modeling studies were performed on crystal structure topoisomerase-I and II along with their co-crystallized ligand (PDB ID:1K4T) and (pdb ID: 5GWK), respectively. Ligands and protein were then prepared using UCSF Chimera by adding hydrogen and assigning Gasteiger charges, then energy minimization. Auto-grid allocated in UCSF-chimera 1.17.3 at the macromolecule center was used to generate the grid box, which was then adjusted to cover the whole protein. Docking was performed using AutoDock Vina. The results were saved as pdbqt and then visualized using Biovia Discovery Studio v21.1.0.20298 [48].

Declarations

Author Contribution Statement

Abdullah A. S. Ahmed and Ibrahim El Tantawy El Sayed suggested the idea and the experimental design; Hanem M. Awad, Abdullah A. S. Ahmed, Yasmine S. Moemen, Mohamed Aly Saad Aly d, Ahmed I. El-Tantawy, and Elshaymaa I. Elmongy performed the experiment and wrote the draft of the manuscript; Hanem M. Awad and Ibrahim El Tantawy El Sayed supervised the implementation of the experiment and analyzed the results. All authors discussed the results and contributed to finalizing the manuscript.

Competing Interests

The authors declare that they have no conflict of interest.

Availability of Data and Materials

All data supporting the findings of this study are available within the paper and its Supplementary Information

Supplementary Material

Spectral data for the characterization of all synthesized compounds were provided in the supplementary material file.

Funding: This research did not receive funding.

References:

1. R.L. Siegel, A.N. Giaquinto and A. Jemal, Cancer Statistics, 2024, *CA: A Cancer J. Clin.*, **74**, 12–49 (2024).
2. R. Kaur, A. Bhardwaj and S. Gupta, Cancer Treatment Therapies: Traditional to Modern Approaches to Combat Cancers, *Mol. Biol. Rep.*, **50**, 9663–9676 (2023).
3. V. Schirrmacher, From Chemotherapy to Biological Therapy: A Review of Novel Concepts to Reduce the Side Effects of Systemic Cancer Treatment, *Int. J. Oncol.*, **54**, 407–419 (2019).
4. S. Datta, D. Choudhury, A. Das, D.D. Mukherjee, M. Dasgupta, S. Bandopadhyay and G. Chakrabarti, Autophagy Inhibition with Chloroquine Reverts Paclitaxel Resistance and Attenuates Metastatic Potential in Human Nonsmall Lung Adenocarcinoma A549 Cells via ROS Mediated Modulation of Beta-Catenin Pathway, *Apoptosis*, **24**, 414–433 (2019).
5. L. Zhong, Y. Li, L. Xiong, W. Wang, M. Wu, T. Yuan, W. Yang, C. Tian, Z. Miao, T. Wang and S. Yang, Small Molecules in Targeted Cancer Therapy: Advances, Challenges, and Future Perspectives, *Signal Transduct. Target. Ther.*, **6**, 201 (2021).
6. E.N. Kuipers, A.D. Dam, N.M. Held, I.M. Mol, R.H. Houtkooper, P.C. Rensen and M.R. Boon, Quercetin Lowers Plasma Triglycerides Accompanied by White Adipose Tissue Browning in Diet-Induced Obese Mice, *Int. J. Mol. Sci.*, **19**, 1786 (2018).
7. P. Martins, J. Jesus, S. Santos, L.R. Raposo, C. Roma-Rodrigues, P.V. Baptista and A.R. Fernandes, Heterocyclic Anticancer Compounds: Recent Advances and the Paradigm Shift Towards the Use of Nanomedicine's Tool Box, *Molecules*, **20**, 16852–16891 (2015).
8. M.A. Abd Eldaim, E. Tousson, I.E. El Sayed, A.Z. Abd Elmaksoud and A.A. Ahmed, Ameliorative Effects of 9-Diaminoacridine Derivative against Ehrlich Ascites Carcinoma–Induced Hepatorenal Injury in Mice, *Environ. Sci. Pollut. Res.*, **28**, 21835–21850 (2021).
9. N. Altwaijry, S. El-Ghlban, I.E. El Sayed, M. El-Bahnsawye, A.I. Bayomi, R.M. Samaka, E. Shaban, E.I. Elmongy, T.A. El-Masry, H.M. Ahmed and N.G. Attallah, In Vitro and In Vivo Antitumor Activity of Indolo[2,3-b]quinolines, Natural Product Analogs from Neocryptolepine Alkaloid, *Molecules*, **26**, 754 (2021).
10. E.I. Elmongy, A.A. Ahmed, I.E. El Sayed, G. Fathy, H.M. Awad, A.U. Salman and M.A. Hamed, Synthesis, Biocidal and Antibiofilm Activities of New Isatin–Quinoline Conjugates against Multidrug-Resistant Bacterial Pathogens along with Their In Silico Screening, *Antibiotics*, **11**, 1507 (2022).
11. C. Nitsche and C.D. Klein, Aqueous Microwave-Assisted One-Pot Synthesis of N-Substituted Rhodanines, *Tetrahedron Lett.*, **53**, 5197–5201 (2012).

12. S.M. Mousavi, M. Zarei, S.A. Hashemi, A. Babapoor and A.M. Amani, A Conceptual Review of Rhodanine: Current Applications of Antiviral Drugs, Anticancer and Antimicrobial Activities, *Artif. Cells Nanomed. Biotechnol.*, **47**, 1132–1148 (2019).
13. J. Szczepański, H. Tuszewska and N. Trotsko, Anticancer Profile of Rhodanines: Structure–Activity Relationship (SAR) and Molecular Targets — A Review, *Molecules*, **27**, 3750 (2022).
14. J. da Silva Santos, J.J. Junior and F.M. da Silva, 1,3-Thiazolidin-4-ones: Biological Potential, History, Synthetic Development and Green Methodologies, *Curr. Org. Synth.*, **15**, 1109–1123 (2018).
15. B. El-Aarag, E.S. Shalaan, A.A. Ahmed, I.E. Tantawy El Sayed and W.M. Ibrahim, Cryptolepine Analog Exhibits Antitumor Activity against Ehrlich Ascites Carcinoma Cells in Mice via Targeting Cell Growth, Oxidative Stress, and PTEN/Akt/mTOR Signaling Pathway, *Anti-Cancer Agents Med. Chem.*, **24**, 436–442 (2024).
16. N. Wang, K.J. Wicht, L. Wang, W.J. Lu, R. Misumi, M.Q. Wang, A.A. El Gokha, M. Kaiser, I.E. El Sayed, T.J. Egan and T. Inokuchi, Synthesis and In Vitro Testing of Antimalarial Activity of Non-Natural-Type Neocryptolepines: Structure–Activity Relationship Study of 2,11- and 9,11-Disubstituted 6-Methylindolo[2,3-b]quinolines, *Chem. Pharm. Bull.*, **61**, 1282–1290 (2013).
17. A.A. Sebeka, A.M. Osman, I.E. El Sayed, M. El Bahanasawy and M.A. Tantawy, Synthesis and Antiproliferative Activity of Novel Neocryptolepine-Hydrazides Hybrids, *J. Appl. Pharm. Sci.*, **7**, 9–15 (2017).
18. N. Wang, M. Świtalska, L. Wang, E. Shaban, M.I. Hossain, I.E. El Sayed, J. Wietrzyk and T. Inokuchi, Structural Modifications of Nature-Inspired Indoloquinolines: A Mini Review of Their Potential Antiproliferative Activity, *Molecules*, **24**, 2121 (2019).
19. I.E. El Sayed, S. Ullah, O.A. Al-Hartomy, A.M. Hasanein, A.A. Ahmed, K.A. Kahilo and M.E. El-Naggar, Synthesis, Nanoformulations, and In Vitro Anticancer Activity of N-Substituted Side Chain Neocryptolepine Scaffolds, *Molecules*, **27**, 1024 (2022).
20. S.F. Abd Elrahman, A.A. Ahmed, D. Abd Elsatar, S. Elkady, A. Elgendy, F. Alnakeeb, E.I. Elmongy, H.A. Henidi, S.M. El-Gendy, I.E. El Sayed and A.A. El-Gokha, Cytotoxic Potential of Novel Quinoline Derivative: 11-(1,4-Bisaminopropylpiperazinyl) 5-Methyl-5H-indolo[2,3-b]quinoline against Different Cancer Cell Lines via Activation and Deactivation of the Expression of Some Proteins, *Int. J. Mol. Sci.*, **24**, 14336 (2023).
21. E.T. Nagy, A.A. Ahmed, E.I. Elmongy, S.M. El-Gendy, I. Elmadbouh, I.E. El Sayed, M.A. Abd Eldaim and A.A. El-Gokha, Design and Cytotoxic Evaluation via Apoptotic and Antiproliferative Activity for Novel 11-(4-Aminophenylamino) Neocryptolepine on Hepatocellular and Colorectal Cancer Cells, *Apoptosis*, **28**, 653–668 (2023).

22. A.A. Ahmed, H.M. Awad, I.E. El-Sayed and A.A. El Gokha, Synthesis and Antiproliferative Activity of New Hybrids Bearing Neocryptolepine, Acridine and Alpha-Aminophosphonate Scaffolds, *J. Iran. Chem. Soc.*, **17**, 1211–1221 (2020).
23. R.R. Neiber, A.A. Galhoum, I.E. El Sayed, E. Guibal, J. Xin and X. Lu, Selective Lead(II) Sorption Using Aminophosphonate-Based Sorbents: Effect of Amine Linker, Characterization and Sorption Performance, *Chem. Eng. J.*, **442**, 136300 (2022).
24. M. Abdeen, M. Hamed, A. Aleem, I. Nassar and I. El-Sayed, A Comparative Study of Metal-Catalyzed Three-Component Synthesis of Alpha-Aminophosphonates, *Curr. Chem. Lett.*, **10**, 221–234 (2021).
25. R.R. Neiber, N.A. Samak, J. Xing, E.I. Elmongy, A.A. Galhoum, I.E. El Sayed, E. Guibal, J. Xin and X. Lu, Synthesis and Molecular Docking Study of Alpha-Aminophosphonates as Potential Multi-Targeting Antibacterial Agents, *J. Hazard. Mater.*, **465**, 133203 (2024).
26. A. Amira, Z. Aouf, H. K'tir, Y. Chemam, R. Ghodbane, R. Zerrouki and N.E. Aouf, Recent Advances in the Synthesis of Alpha-Aminophosphonates: A Review, *ChemistrySelect*, **6**, 6137–6149 (2021).
27. P.R. Varga and G. Keglevich, The Last Decade of Optically Active Alpha-Aminophosphonates, *Molecules*, **28**, 6150 (2023).
28. L. Oniciuc, D. Amăriucăi-Mantu, D. Diaconu, V. Mangalagiu, R. Danac, V. Antoci and I.I. Mangalagiu, Benzoquinoline Derivatives: An Attractive Approach to Newly Small Molecules with Anticancer Activity, *J. Enzyme Inhib. Med. Chem.*, **24**, 8124 (2023).
29. Y. Bansal and O. Silakari, Multifunctional Compounds: Smart Molecules for Multifactorial Diseases, *Eur. J. Med. Chem.*, **76**, 31–42 (2014).
30. C.B. Sangani, J.A. Makawana, X. Zhang, S.B. Teraiya, L. Lin and H.L. Zhu, Design, Synthesis and Molecular Modeling of Pyrazole–Quinoline–Pyridine Hybrids as a New Class of Antimicrobial and Anticancer Agents, *Eur. J. Med. Chem.*, **76**, 549–557 (2014).
31. M. Badr, E.I. Elmongy, D. Elkhateeb, Y.S. Moemen, A. Khalil, H. Ali, R. Binsuwaidan, F. Awadallah and I.E. El Sayed, In Silico and In Vitro Investigation of Cytotoxicity and Apoptosis of Acridine/Sulfonamide Hybrids Targeting Topoisomerases I and II, *Pharmaceuticals*, **17**, 1487 (2024).
32. W.J. Lu, K.J. Wicht, L. Wang, K. Imai, Z.W. Mei, M. Kaiser, I.E. El Sayed, T.J. Egan and T. Inokuchi, Synthesis and Antimalarial Testing of Neocryptolepine Analogues: Addition of Ester Function in SAR Study of 2,11-Disubstituted Indolo[2,3-b]quinolines, *Eur. J. Med. Chem.*, **64**, 498–511 (2013).
33. I. El Sayed, P. Van der Veken, K. Steert, L. Dhooghe, S. Hostyn, G. Van Baelen, G. Lemiere, B.U. Maes, P. Cos, L. Maes and J. Joossens, Synthesis and Antiplasmodial Activity of

Aminoalkylamino-Substituted Neocryptolepine Derivatives, *J. Med. Chem.*, **52**, 2979–2988 (2009).

34. M. El-Bahnsawye, M.K. Hussein, E.I. Elmongy, H.M. Awad, A.A. Tolan, Y.S. Moemen, A. El-Shaarawy and I.E. El-Sayed, Design, Synthesis, and Antiproliferative Activity of Novel Neocryptolepine–Rhodanine Hybrids, *Molecules*, **27**, 7599 (2022).
35. E. Hejchman, H. Kruszewska, D. Maciejewska, B. Sowirka-Taciak, M. Tomczyk, A. Sztok, J. Sz-Ignasiak, J. Jankowski and I. Młynarczuk-Biały, [title not provided], *Monatsh. Chem.*, **150**, 255–266 (2019).
36. A.M. Hassan, A.O. Said, B.H. Heakal, A. Younis, W.M. Aboulthana and M.F. Mady, Green Synthesis, Characterization, Antimicrobial and Anticancer Screening of New Metal Complexes Incorporating Schiff Base, *ACS Omega*, **7**, 32418–32431 (2022).
37. M.S. Ayoup, R.A. Rabee, H. Abdel-Hamid, M.F. Harras, N.G. El Menofy and M.I. Ismail, Exploration of Nitroaromatic Antibiotics via Sanger's Reagent: Synthesis, In Silico, and Antimicrobial Evaluation, *ACS Omega*, **7**, 5254–5263 (2022).
38. E.M. Flefel, W.A. El-Sayed, A.M. Mohamed, W.I. El-Sofany and H.M. Awad, Synthesis and Anticancer Activity of New 1-Thia-4-azaspiro[4.5]decane, Their Derived Thiazolopyrimidine and 1,3,4-Thiadiazole Thioglycosides, *Molecules*, **22**, 170 (2017).
39. B.L. Staker, M.D. Feese, M. Cushman, Y. Pommier, D. Zembower, L. Stewart and A.B. Burgin, Structures of Three Classes of Anticancer Agents Bound to the Human Topoisomerase I−DNA Covalent Complex, *J. Med. Chem.*, **48**, 2336–2345 (2005).
40. R. Chen, L. Huo, Y. Jaiswal, J. Huang, Z. Zhong, J. Zhong, L. Williams, X. Xia, Y. Liang and Z. Yan, Design, Synthesis, Antimicrobial, and Anticancer Activities of Acridine Thiosemicarbazides Derivatives, *Molecules*, **24**, 2065 (2019).
41. S.S. Butt, Y. Badshah, M. Shabbir and M. Rafiq, Molecular Docking Using Chimera and AutoDock Vina Software for Nonbioinformaticians, *JMIR Bioinform. Biotechnol.*, **1**, e14232 (2020).
42. S. Khaerunnisa, H. Kurniawan, R. Awaluddin, S. Suhartati and S. Soetjipto, Potential Inhibitor of COVID-19 Main Protease (Mpro) from Several Medicinal Plant Compounds by Molecular Docking Study, *Preprints*, 2020030226 (2020).
43. A. Pantos, I. Tsogas and C.M. Paleos, Guanidinium Group: A Versatile Moiety Inducing Transport and Multicompartmentalization in Complementary Membranes, *Biochim. Biophys. Acta, Biomembr.*, **1778**, 811–823 (2008).
44. N. Zidar, T. Tomašić, R. Sink, V. Rupnik, A. Kovac, S. Turk, D. Patin, D. Blanot, C. Contreras Martel, A. Dessen and M. Müller Premru, Discovery of Novel 5-Benzylidenerhodanine and 5-

Benzylidenethiazolidine-2,4-dione Inhibitors of MurD Ligase, *J. Med. Chem.*, **53**, 6584–6594 (2010).

45. G. Indrayanto, G.S. Putra and F. Suhud, Validation of In-Vitro Bioassay Methods: Application in Herbal Drug Research, *Profiles Drug Subst. Excip. Relat. Methodol.*, **46**, 273–307 (2021).
46. A. Chaurasyia, P. Chawla, V. Monga and G. Singh, [title not provided], *Chem. Biol. Drug Des.*, **101**, 500–549 (2023).
47. L.B. Saltz, J.V. Cox, C. Blanke, L.S. Rosen, L. Fehrenbacher, M.J. Moore, J.A. Maroun, S.A. Ackland, P.K. Locker, N. Pirotta and G.L. Elfring, Irinotecan Plus Fluorouracil and Leucovorin for Metastatic Colorectal Cancer, *N. Engl. J. Med.*, **343**, 905–914 (2000).
48. G.M. Longo, S. Sayols, M.E. Stefanova, T. Xie, W. Elsayed, A. Panagi, A.I. Stavridou, G. Petrosino, E. Ing-Simmons, U.S. Melo and H.J. Gothe, Type II Topoisomerases Shape Multi-Scale 3D Chromatin Folding in Regions of Positive Supercoils, *Mol. Cell*, **84**, 4267–4281 (2024).

Supplementary Files

This is a list of supplementary files associated with this preprint. Click to download.

- SupplementaryFile.pdf